

# **pH-Responsive Aloe Vera Hydrogels Loaded with Imatinib for Targeting Drug Resistance in Cancer**



By

Aroob Hasan Khan

(Registration No: 00000401953)

Department of Biomedical Sciences

School of Mechanical and Manufacturing Engineering

National University of Sciences & Technology (NUST)

Islamabad, Pakistan

(2024)

# **pH-Responsive Aloe Vera Hydrogels Loaded with Imatinib for Targeting Drug Resistance in Cancer**



By

Aroob Hasan Khan

(Registration No: 00000401953)

A thesis submitted to the National University of Sciences and Technology, Islamabad,

in partial fulfillment of the requirements for the degree of

**Master of Science in  
Biomedical Sciences**

Supervisor: Dr. Adeeb Shehzad

School of Mechanical and Manufacturing Engineering

National University of Sciences & Technology (NUST)

Islamabad, Pakistan

(2024)

## THESIS ACCEPTANCE CERTIFICATE

Certified that final copy of MS/MPhil thesis written by **RegnNo. 00000401953 Aroob Hasan Khan** of **School of Mechanical & Manufacturing Engineering (SMME)** has been vetted by undersigned, found complete in all respects as per NUST Statues/Regulations, is free of plagiarism, errors, and mistakes and is accepted as partial fulfillment for award of MS/MPhil degree. It is further certified that necessary amendments as pointed out by GEC members of the scholar have also been incorporated in the said thesis titled. **pH-responsive AleoVera Hydrogels Loaded with Imatinib for Targeting Drug Resistance in Cancer**

Signature:



Name (Supervisor): Adeeb Shehzad

Date: 13 - Aug - 2024

Signature (HOD):



Date: 13 - Aug - 2024

Signature (DEAN):



Date: 13 - Aug - 2024



**National University of Sciences & Technology (NUST)**  
**MASTER'S THESIS WORK**

We hereby recommend that the dissertation prepared under our supervision by: Aroob Hasan Khan (00000401953)  
Titled: pH-responsive AleoVera Hydrogels Loaded with Imatinib for Targeting Drug Resistance in Cancer be accepted in partial fulfillment of the requirements for the award of MS in Biomedical Sciences degree.

**Examination Committee Members**

- |    |                           |            |
|----|---------------------------|------------|
| 1. | Name: Aneeqa Noor         | Signature: |
| 2. | Name: Muhammad Asim Waris | Signature: |
| 3. | Name: Waheed Miran        | Signature: |
- Supervisor:** Adeeb Shehzad  
Signature:   
Date: 13 - Aug - 2024

Head of Department

13 - Aug - 2024

Date

**COUNTERSIGNED**

13 - Aug - 2024

Date

Dean/Principal

---

## CERTIFICATE OF APPROVAL

This is to certify that the research work presented in this thesis, entitled “pH-Responsive Aloe Vera Hydrogels Loaded with Imatinib for Targeting Drug Resistance in Cancer” was conducted by Ms. Aroob Hasan Khan, under the supervision of Dr. Adeeb Shehzad

No part of this thesis has been submitted anywhere else for any other degree. This thesis is submitted to the Department of Biomedical Engineering and Sciences (BMES) in partial fulfillment of the requirements for the degree of Master of Science in the Field of MS Biomedical Sciences, Department of School of Mechanical and Manufacturing Engineering (SMME) National University of Sciences and Technology, Islamabad.


Student Name: Aroob Hasan Khan

Signature:  \_\_\_\_\_

Supervisor Name: Dr. Adeeb Shehzad

Signature:  \_\_\_\_\_

Name of Dean/HOD: Dr. Muhammad Asim Waris

Signature:  \_\_\_\_\_

## **AUTHOR'S DECLARATION**

I Aroob Hasan Khan hereby state that my MS thesis titled “pH-Responsive Aloe Vera Hydrogels Loaded with Imatinib for Targeting Drug Resistance in Cancer” is my own work and has not been submitted previously by me for taking any degree from the National University of Sciences and Technology, Islamabad or anywhere else in the country/ world.

At any time if my statement is found to be incorrect even after I graduate, the university has the right to withdraw my MS degree.

Name of Student: Aroob Hasan Khan


Date: 13/08/2024

## **PLAGIARISM UNDERTAKING**

I solemnly declare that the research work presented in the thesis titled “pH-Responsive Aloe Vera Hydrogels Loaded with Imatinib for Targeting Drug Resistance in Cancer” is solely my research work with no significant contribution from any other person. Small contribution/ help wherever taken has been duly acknowledged and that complete thesis has been written by me.

I understand the zero tolerance policy of the HEC and the National University of Sciences and Technology (NUST), Islamabad towards plagiarism. Therefore, I as an author of the above titled thesis declare that no portion of my thesis has been plagiarized and any material used as reference is properly referred to/cited.

I undertake that if I am found guilty of any formal plagiarism in the above titled thesis even after the award of MS degree, the University reserves the right to withdraw/revoke my MS degree and that HEC and NUST, Islamabad have the right to publish my name on the HEC/University website on which names of students are placed who submitted plagiarized thesis.

Student Signature:  \_\_\_\_\_

Name: Aroob Hasan Khan

*To my parents and grandparents*



## ACKNOWLEDGEMENTS

In the name of Allah, the Most Gracious, the Most Merciful. First and foremost, would thank Allah Almighty for His countless blessings and guidance throughout the journey of my research work. This accomplishment of mine would have been impossible without His Grace.

I am deeply honored to be supervised by Dr. Adeb Shehzad, Associate Professor, Department of Biomedical Sciences & Engineering, SMME, NUST, and highly grateful for his invaluable support, words of encouragement, and guidance. Without his expertise and knowledge, I wouldn't have been successful in the completion of my research work. My deep appreciation and gratitude go to my GEC members, Dr. Aneeqa Noor, Dr. Asim Waris, and Dr. Waheed Miran for their guidance, support, and constructive feedback throughout the journey.

My sincere thanks to my friends, lab mates, and seniors for providing unconditional support, and assistance and being a source of motivation every day, and for stimulating an environment that helped me learn and grow.

Lastly, I am eternally indebted to my family, parents, and grandparents for their endless patience, understanding, and support towards me. Their faith encouraged me to achieve this milestone. I would also like to thank anyone who contributed and assisted, directly and indirectly in the completion of my thesis. Thank you all for your endless support and encouragement.

## TABLE OF CONTENTS

<b>ACKNOWLEDGEMENTS</b>	<b>VIII</b>
<b>TABLE OF CONTENTS</b>	<b>IX</b>
<b>LIST OF TABLES</b>	<b>XII</b>
<b>LIST OF FIGURES</b>	<b>XIII</b>
<b>LIST OF EQUATIONS</b>	<b>XIV</b>
<b>LIST OF SYMBOLS, ABBREVIATIONS AND ACRONYMS</b>	<b>XV</b>
<b>ABSTRACT</b>	<b>XVI</b>
<b>CHAPTER 1: INTRODUCTION</b>	<b>17</b>
<b>1.1. Problem Statement</b>	<b>19</b>
<b>1.2. Aims and Objectives</b>	<b>19</b>
<b>1.3 Research Rationale</b>	<b>20</b>
<b>1.4 Research Approach</b>	<b>20</b>
<b>CHAPTER 2: LITERATURE REVIEW</b>	<b>22</b>
<b>2.1. Epidemiology of Cancer</b>	<b>22</b>
<b>2.2 Hydrogel Properties</b>	<b>23</b>
2.2.1 pH Sensitivity	25
2.2.2. Crosslinking	27
<b>2.3 The Tumor Microenvironment (TME) and Pathways Mutated</b>	<b>28</b>
<b>2.4 Imatinib</b>	<b>29</b>
<b>2.5. Drug Resistance</b>	<b>30</b>
<b>2.6 Aloe Vera</b>	<b>32</b>
2.6.1. Aloe vera Hydrogels	34
2.6.2 Properties of Aloe Vera Hydrogels	35
<b>2.7. Scope of the Study:</b>	<b>36</b>

<b>CHAPTER 3: MATERIALS AND METHODOLOGY</b>	<b>37</b>
<b>3.1 Materials</b>	<b>37</b>
3.1.1 Equipment	37
3.1.2 Reagents/Chemicals	38
3.1.3 Solutions Used for Hydrogel Synthesis	39
3.1.4 Solutions used for swelling, degradation, and release profiling	39
3.1.5 Solutions used for cell culture	40
<b>3.2. Methodology</b>	<b>40</b>
3.2.1 Aloe vera gel extraction	40
3.2.2 Synthesis of hydrogel	41
3.2.3 Characterizations	43
3.2.4 Physiochemical Analysis	44
3.2.5 Antioxidant Activity	46
3.2.6 Biocompatibility	46
3.2.7 Cell viability	47
3.2.7 Statistical Analysis	48
<b>CHAPTER 4: RESULTS</b>	<b>49</b>
<b>4.1 Characterization</b>	<b>49</b>
4.1.1 FT-IR	49
4.1.2 SEM	50
4.1.3 Elemental Analysis:	51
<b>4.2 Physiochemical Analysis</b>	<b>52</b>
4.2.1 Swelling Analysis	52
4.2.2 Gel Fraction	54
4.2.3 In-vitro degradation	55

4.2.4 Encapsulation Efficiency of AV hydrogel	57
4.2.5 Drug Release	57
<b>4.3 Antioxidant Analysis</b>	<b>59</b>
<b>4.4 Biocompatibility Assay</b>	<b>60</b>
<b>4.5 Cell Viability</b>	<b>61</b>
<b>CHAPTER 5: DISCUSSION</b>	<b>63</b>
<b>CHAPTER 6: CONCLUSION AND FUTURE PROSPECTS</b>	<b>69</b>
<b>REFERENCES</b>	<b>70</b>

## LIST OF TABLES

Table 2.1 Recently reported applications of hydrogels and their use in DDS .....	24
Table 2.2 Compounds found in Aloe Vera and their advantages.....	32
Table 3.1 List of equipment used during the study and their manufacturers.....	37
Table 3.2 List of chemicals used in the study and their manufacturers.....	38
Table 3.3 Solutions Prepared for Hydrogel Synthesis.....	39
Table 3.4 Solutions Prepared for Physiochemical Analysis .....	39
Table 3.5 Solutions prepared for cell culture viability activity.....	40
Table 3.6 Hydrogel Composition .....	42
Table 4.1 IM encapsulation efficiency of PVA/SA and PVA/SA/AV.....	57

## LIST OF FIGURES

	<b>Page No.</b>
Figure 1.1 Flowchart of Research Approach .....	21
Figure 2.1 pH dependant swelling of hydrogel matrix.....	27
Figure 2.2 The tumor microenvironment and its associated factors .....	29
Figure 2.3 Demonstrates the mechanism of action of anticancer agent.....	30
Figure 2.4 Different mechanisms of resistance to IM in cancer cells. ....	31
Figure 3.1 Steps in the extraction of AV gel and the formation of AV hydrogel....	43
Figure 4.1 FT-IR spectra .....	50
Figure 4.2 SEM Images. ....	51
Figure 4.3 EDX .....	52
Figure 4.4 Swelling Analysis .....	54
Figure 4.5 Gel fraction .....	55
Figure 4.6 Degradation Analysis .....	56
Figure 4.7 Drug Release .....	58
Figure 4.8 Absorbance curve and R-squared value of IM at 260nm .....	59
Figure 4.9 Antioxidant Activity .....	60
Figure 4.10 Hemolytic Activity .....	61
Figure 4.11 Cell Viability.....	62

## LIST OF EQUATIONS

<i>Swelling %</i>	<a href="#">Eq. 1</a> .....	44
<i>Gel Fraction %</i>	<a href="#">Eq. 2</a> .....	44
<i>Degradation %</i>	<a href="#">Eq. 3</a> .....	45
<i>Encapsulation Efficiency %</i>	<a href="#">Eq. 4</a> .....	45
<i>Drug Release %</i>	<a href="#">Eq. 5</a> .....	46
<i>Scavenging Activity %</i>	<a href="#">Eq. 6</a> .....	46
<i>Hemolysis %</i>	<a href="#">Eq. 7</a> .....	47
<i>Cell Conc. (cells/ml)</i>	<a href="#">Eq. 8</a> .....	47
<i>Cell viability %</i>	<a href="#">Eq. 9</a> .....	48

## LIST OF SYMBOLS, ABBREVIATIONS AND ACRONYMS

AA	Acrylic Acid
AV	Aloe Vera
PVA	Poly Vinyl Alcohol
SA	Sodium Alginate
IM	Imatinib
FT-IR	Fourier Transform Infrared
SEM	Scanning Electron Microscopy
EDX	Energy Dispersive X-Ray
MCF-7	Breast Cancer Cell Lines



## ABSTRACT

Cancer and its reoccurrence have become a major health problem affecting the quality of life for millions of individuals every year. The currently available strategies, radiotherapy, and chemotherapy have non-specific targets, lower solubility, and severe side effects. Hydrogels are crosslinked polymeric networks with higher swelling properties, degradation, biocompatibility, and flexibility which can be manipulated based on the desired application. Incorporating AV can elevate the antioxidant, and anticancer properties of the hydrogel based drug delivery system (DDS) also warranting enhanced swelling, drug release, and environmental degradability of the system. Acrylic acid (AA) induces pH-responsive properties in the hydrogels. The PVA/SA and PVA/SA/AV hydrogels were synthesized with a pH responsive behavior and investigated at different pH conditions. The unloaded and loaded PVA/SA and PVA/SA/AV hydrogels with imatinib (IM) were characterized for their structural morphology, physiochemical characteristics, and antioxidant and anticancer activity. The IM loaded PVA/SA/AV hydrogels showed increased pore size in SEM micrographs, enhanced swelling abilities up to 400%, 100% degradation, 56% encapsulation efficiency, and drug release profiles of up to 94% in 24 h, compared to PVA/SA hydrogels loaded with IM. Dpph radical scavenging activity was also observed to be enhanced in PVA/SA/AV hydrogels. Finally, the cell viability analysis in resistant MCF-7 breast cancer cell lines exhibited 41% cell viability of the PVA/SA/AV hydrogels loaded with IM implying a promising potential of AV to be incorporated in a hydrogel based drug delivery system for targeting drug resistance in cancer.

**KEYWORDS:** Aloe Vera, Breast Cancer, Degradation, Dpph, Drug Release, Drug Resistance, Imatinib, MTT, pH responsive, Swelling.

## CHAPTER 1: INTRODUCTION

Cancer is characterized by the aberrant proliferation leading to metastasis of the cancerous cells inside the body, resulting from the combination of exposure to various environmental factors, and genetic mutations (Cairns, 1975). Cancer and its reoccurrence have become a major health problem affecting the quality of life for millions of individuals every year (Mehlen & Puisieux, 2006; Sepantafar et al., 2017). The currently available strategies, radiotherapy, and chemotherapy have non-specific targets and with lower solubility, they cause severe side effects (Tian, Chen, & Niu, 2014). Chemotherapy is a widely used approach in cancer therapy which involves delivering cytotoxic drugs to target cancer cells, however, these highly toxic drugs are poorly specific and target both the normal and cancerous cells. As the chemotherapeutic drug is administered systemically, the drug content peaks and declines rapidly, producing inadequate therapeutic effects. As a result, the drug is required to be administered repeatedly, causing adverse side reactions. Additionally, since the drug is administered systemically, a maximum fraction of the drug is highly likely to be lost in the bloodstream, before reaching the site of action. Two other modes of therapy, hormonal therapy, and immunotherapy are also being investigated currently for the treatment of cancer, however, they also come with limitations in their applications (Ta, Dass, & Dunstan, 2008). Radiation therapy uses X-rays to puncture through the DNA of cancerous cells inhibiting growth and proliferation but also targets the normal cells surrounding the cancer cells leading to side effects (Mohan et al., 2019). Common immediate side effects include; nausea, fatigue, erythema, and even neurological pain, followed by long-term side effects (Birgisson, Pålman, Gunnarsson, & Glimelius, 2007).

Owing to these obstacles, new techniques are being tested for more controlled, effective, and localized release of therapeutic drugs as alternatives to systemically administered drugs. Drug delivery systems assembled using hydrogels, polymers, liposomes, nanoparticles, and micelles are being investigated widely for drug loading efficiency, biodegradability, biocompatibility, and drug release (Tian et al., 2014). Respectively, ‘smart hydrogels’ have received considerable attention for a more controlled and localized release of chemotherapeutic drugs. These drugs are loaded into these systems by passive absorption or

direct addition into the formulations. Drug loading efficiency is still a limitation in these formulations while the implants require additional costs for insertion. Due to these reasons, most cancer research has now been oriented toward polymer-based injectable hydrogel formulations that are biocompatible, degradable, cost-effective, have low toxicity, are naturally available, and antibacterial with efficient drug loading and release properties (Khani et al., 2022; Ta et al., 2008). These optimizable hydrogel formulations exhibit a more controlled release of the drug, lowering exposure to healthy cells. Previously, hydrogels have been researched in tumor imaging, prostheses, tissue replacement, etc. Presently, the physiochemical and biochemical characteristics of the hydrogels are being modified in accordance with the complexity of the tumor microenvironment and undesirable side effects on healthier cells for the purpose of cancer research (Kim, Kim, Chun, Lee, & Song, 2012; Sepantafar et al., 2017).

Hydrogels at the core are crosslinked networks of synthetic, natural, or semi-synthetic polymers. These hydrogels have higher swelling properties, degradation, biocompatibility, and even the flexibility for efficient manipulation for desired use. As a result, hydrogels have great potential to be explored in cancer research including studying underlying mechanisms, diagnostics, and therapeutics (Ahmed, 2015; Park, Lewis, & Gerecht, 2017; Zhu & Marchant, 2011). According to certain studies, the high water-retaining property of the polymer networks serves as efficient drug reservoirs. In contrast to the systemic administration, hydrogels result in localized and concentrated release inside the tumors avoiding off-target release of the drug and reducing adverse effects (Pacheco, Baiao, Ding, Cui, & Sarmiento, 2023).

Aloe Vera (AV) also known as *Aloe Barbadensis* (miller) is one of the most widely used plants in medicine and dermatology. The interesting pharmaceutical properties like antioxidant, anti-inflammatory, biocompatibility, and antimicrobial activities result from AV's polysaccharides composition. AV incorporation strengthens the physiochemical properties of the hydrogel drug delivery system also warranting the environmental degradability of the system (Klein & Penneys, 1988; Sánchez-Machado, López-Cervantes, Sendón, Sanches-Silva, & Technology, 2017; Wang et al., 2021). The various bioactive compounds found in AV have uses in cosmetics, food and in the medical industry (dermatology, wound healing, anti-

diabetic, anti-cancerous, anti-oxidant, anti-inflammatory, etc.) (Balaji et al., 2015). On the other hand, polyvinyl alcohol (PVA) incorporation further intensifies the structural, temperature, and pH stability properties (Rivera-Hernández, Antunes-Ricardo, Martínez-Morales, & Sanchez, 2021). Side by side, the cancerous cells inside the body maintain an acidic pH of around 5 to 6.5 while the healthy cells maintain a neutral pH of around 7.4 (Nasef, Khozemy, & Mahmoud, 2023). The introduction of acrylic acid (AA) induces pH-responsive properties in the hydrogels (Sullad, Manjeshwar, Aminabhavi, & Research, 2010). The pH-responsive hydrogels are being studied for their effective drug delivery designs and many studies report great potential.

Realizing the potential of the pH-responsive behavior of hydrogels, our study puts in efforts to contribute to this field by exploring the effects of introducing the antioxidant, antimicrobial, and anti-cancerous properties of AV into hydrogels for drug delivery to tumor sites.

### **1.1. Problem Statement**

Cancer incidence is a major challenge in developing countries, like Pakistan with the second highest mortality rate in South Asian countries. The use of conventional chemotherapeutic drugs kills the cancerous cells and the healthy cells, significantly impacting the patient's immune system. Additionally, the development of drug resistance due to early exposure to the drug in the body's systemic circulation induces mutations and resistance toward the administered drug. Chemotherapeutic drugs in themselves are costly, and combining them with a non-cost-effective drug delivery system is a problem for developing countries like Pakistan. Developing a cost-effective, biocompatible, biodegradable, and easily up-scalable DDS that offers site specific delivery to the cancerous cells has become highly inevitable.

### **1.2. Aims and Objectives**

- Synthesis of Aloe Vera hydrogel with enhanced structural and physiochemical stability
- The efficient and effective integration of the drug and its pH controlled release

- To improve cancer treatment strategies and reduce drug resistance

### **1.3 Research Rationale**

Drug resistance has made the hunt for the development of improved cancer drug delivery strategies extremely limited with resistant cancer cells being able to escape the chemotherapeutic drugs leading to failure of treatment and cancer progression. Under such circumstances, innovative, cost-effective, and biocompatible drug delivery systems have become essential to surpass these limitations and provide an effective treatment.

AV is a plant that is cultivated worldwide in homes by people, in nurseries, and grown naturally in desert areas and drylands. AV has been explored for centuries in medicine, cosmetics, dermatology, wound healing, and as an anti-allergen. It is non-toxic and has anti-proliferative, anti-diabetic, anti-tumor, anti-microbial, and antioxidant, etc. properties making it an attractive agent for drug delivery applications. It has the flexibility to be modified according to the desired application which enhances its potential to be used as a hydrogel. AV is readily available in Pakistan and cost-effective.

Hydrogels are hydrophilic 3D polymers that can absorb large quantities of water, carry therapeutic agents, or small biomolecules, and deliver them in a controlled manner. Using AV to form the hydrogel, we can develop a system that offers the benefits of AV combined with its cost-effectiveness. A system that can efficiently encapsulate the chemotherapeutic agent and release it in a pH-dependent controlled manner at the targeted tumor site. Our current study will evaluate the applicability of AV hydrogel against drug resistance induced in cancerous cells and their potential in the direction of drug delivery systems

### **1.4 Research Approach**

It is proposed that this study will aim at synthesizing a hydrogel with structural reinforcement, biodegradability, and efficient therapeutic loading and release for the treatment of tumor cells. The Imatinib/hydrogel system is to be worked through the characterizations (FTIR, SEM) for structural and functional group analysis, swelling ratio, degradation, and drug release for pH-controlled behavior testing. Once, the system proves to be optimized, it will be worked through anticancer studies to analyze cytotoxicity. Finally, statistical analysis

will be applied to evaluate the efficacy of the loaded and unloaded AV hydrogels. The proposed system promises a great new opportunity to treat cancerous cells with targeted therapy reducing side-effects to healthy cells.

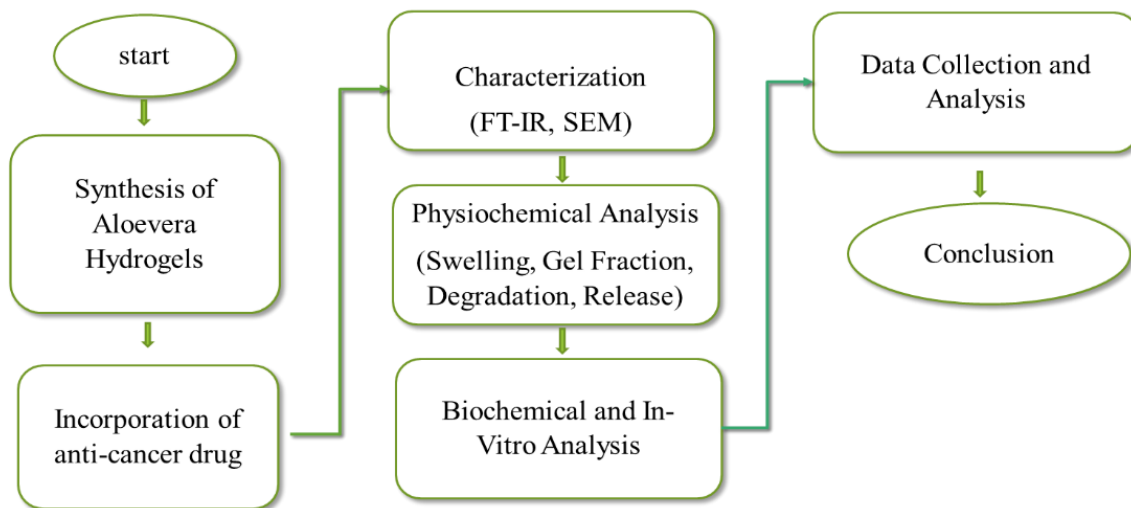


*Figure 1.1 Flowchart of steps to be followed during laboratory work*

## CHAPTER 2: LITERATURE REVIEW

### 2.1. Epidemiology of Cancer

According to cancer statistics, in 2023, about 1.9 million incidences of cancer were alone diagnosed in the U.S. Categorizing based on sex, men have a higher probability of cancer diagnosis, 40.9% compared to women which is 39.1%. This is highly due to factors like smoking, hormones, immune functions, and exposure to more carcinogenic factors in the environment compared to women. Additionally, the highest number of deaths have been reported in men by lung, colorectal cancer, and prostate cancer, while in women lung and breast cancers have resulted in the highest death rate. Lung cancer is the leading cause of mortality in cancer patients, 2.5x and about 81% of these patients have a history of smoking (Siegel, Miller, Wagle, & Jemal, 2023). Compared to other human diseases, cancer is associated with the highest rate of economic, social, and clinical burden on the patients and their caretakers. In an average 74-year lifetime, there's a 20.2% chance of cancer diagnosis, 22.4% in men, and 18.2% in women, when talking sex specifically. Currently, cancer has the highest mortality rate worldwide, and in about 40 years' time, it is likely to become the first (Mattiuzzi, Lippi, & health, 2019).

The International Agency for Research on Cancer's (IARC), study for incidence in Pakistan reports that about 0.18 million new incidences are reported with 0.32 million prevalent cases in the last five years. The cancer related fatalities are 0.11 million. The rate of breast cancer is highest among Pakistani women in Asia with every 1 woman out of 9 facing the risk of developing cancer once in her lifetime, followed by lung, lip, and mouth cancer in males. Smoking, gutka, paan, adulteration, and nutrient deficiencies are some of the biggest risk factors for developing lung, mouth, and lip cancer in Pakistan (Ali et al., 2022). In another study by GLOBOCON, from 2013 to 2018, around 171,152 breast cancer cases were reported which is around 19.58% of total cases, followed by lip and oral cancer which is around 10.58%, and lung cancer at 5.61%. About 117,286 cancer-related deaths were reported with breast cancer at the highest rate at 14%. If we compare this data with other countries in South Asia, Pakistan stands at second place in cancer related mortality rate (Abbas et al., 2020).

## 2.2 Hydrogel Properties

Hydrogels have become an attractive alternative to orthodox therapeutic strategies due to their stimuli-sensitive nature, lower rates of toxicity, variable sol-gel transformation, and enhanced drug loading efficiency and release. A number of interactions; including H-bonding, electrostatic and van der Waals forces, and hydrophobic interactions drive the structural and functional properties of the hydrogels. These interactions within the hydrogels also control the stabilization of drug encapsulation and kinetics of release (Jain, 2020). The microarchitecture of a hydrogel, which represents its polymeric network organization and porosity is influenced by the concentration of polymers used, crosslinking conditions, and the preparation method. The pore size of the system displays a crucial role in mechanical stability. Petite pore sizes or lower porosity inhibit cell proliferation and induce aggregation while larger pores reduce mechanical stability.

Hydrogel microarchitectures are customarily visualized at the nanoscale (surface and cross-section) and characterized through the scanning electron microscopy (SEM) technique. In SEM, a high energy electron beam of primary electrons is directed towards a gold-coated sample, which emits a secondary beam of electrons and backscattered electrons. The secondary electrons provide information about the surface topography while the backscattered electrons give information about the different chemical compositions of the sample. The porosity percentage, pore sizes and distribution, polymeric fiber thickness, and orientation are also visualized. The energy dispersive X-ray (EDX) scan detects the hydrogel elemental composition (Martinez-Garcia et al., 2022).

The hydrogel stability can be deduced by determining their surface charge which tells about their ability to aggregate in the cells or interact with them for their proposed application. The higher is the charge on the surface, the higher are the repulsive interactions that stabilize the hydrogel with a uniform distribution. A  $\pm 30$  mV value is considered stable for the zeta potential (Gonçalves, Pereira, & Gama, 2010).



The biodegradation property of the hydrogel requires it to degrade within a certain period after performing the required task. It modulates drug release over the course of days or weeks and itself gets degenerated inside the system. The process of drug release inside the system involves three main steps; reaching the site of action, matrix swelling, and chemical interaction of the drug/hydrogel system with the site of action. The surface-to-volume ratio is larger for smaller hydrogels, which promotes faster drug release as the drug is situated along the surface while the larger hydrogels tend to incorporate drugs deep inside the core, resulting in slower release. Hydrogel composition and stimuli responsiveness to pH, temperature, and other factors also modulate the release of the anti-cancer agent (Gonçalves et al., 2010).

Drug encapsulation efficiency is achieved through a number of processes; mainly, direct dissolution, desolvation, solvent evaporation, etc. Drug loading efficiency requires encapsulation of the drug without compromising the matrix formed by the polymers and the nature of polymers (molecular weight, solubility, functional groups, drug-polymer compatibility, etc.) (Gonçalves et al., 2010; Pacheco et al., 2023).

Table 2.1 Recently reported applications of hydrogels and their use in DDS for cancer therapy (Dattilo, Patitucci, Prete, Parisi, & Puoci, 2023).

<b>Cancer</b>	<b>Hydrogel Source</b>	<b>Drug Loaded</b>	<b>Cytotoxic Effects</b>
Breast Cancer	Hyaluronic Acid	Doxorubicin	<ul style="list-style-type: none"> <li>•Great anti-cancer activity</li> <li>•Synergistic effects in combination with near-infrared light</li> </ul>
Glioblastoma	Cellulose/Chitosan	TRAIL	<ul style="list-style-type: none"> <li>•Adequate release of TRAIL from hydrogels</li> <li>•Cytotoxic activity existent</li> </ul>
Colorectal	CMC/Alginate	Methotrexate/	<ul style="list-style-type: none"> <li>•Concentration dependent cytotoxicity</li> </ul>

Cancer		Asprin	•10% reduction in cell viability
Lung Cancer	Acylhydrazide CMC	Limonin	•Enhanced tumor suppression •Sustained release of the drug
Hepatocellular Carcinoma	N- Carboxymethyl Chitosan	Doxorubicin	•Good biodegradation •pH responsive •Enhanced cytotoxicity •Reduced rate of side effects
Prostate Cancer	Alginate/cyclode xtrins	Paclitaxel	•Dose dependent release of the drug •Decreased metabolic activity of cancer cells
Renal Cell Carcinoma	K- Carrageenan/Chi tosan	Sunitinib	•pH dependent release

### 2.2.1 pH Sensitivity

The different regions of the human body exhibit variations in their pH, with tumor microenvironments ranging from 5.8 to 7.2 (due to aerobic glycolysis) while the normal cells exhibit a pH of 7.4. These variations have resulted in the formation of site specific pH responsive hydrogels that are biocompatible, release drugs, and degrade in an acidic environment (Sun, Song, Wang, Hu, & Wu, 2019). Such hydrogels exhibit swelling depending on the pH of the action site due to the variations in the interactions in their hydrophobic or hydrophilic bonds in the polymer matrix and their non-covalent interactions (Jacob et al., 2021). In the backbones and sidechains of these polymers, ionizable groups are present which can either get protonated or deprotonated by changing the conformation of their acidic groups or anionic (carboxyl groups -COOH) or basic groups or cationic (ammonia –

NH<sub>2</sub>) in reaction to the environmental change in pH. Such hydrogels with chemotherapeutic drug loading are developed by conjugating their acid-cleavable bonds. Consequently, at the physiological pH (7.4) of the normal cells, they show no pharmaceutical activity but release the drug in the acidic tumor microenvironment reducing systemic toxicity and improving treatment efficacy (Sun et al., 2019).

The sidechains, either basic or acidic have pK<sub>a</sub> and pK<sub>b</sub> values which affect the swelling of the hydrogel based on the environmental pH. In the acidic species, when the pH is higher than the pK<sub>a</sub>, formation of positive and negative charges in the solution and the polymer matrix occurs. While, in basic species, ionization in the polymer matrix occurs if the environmental pH is less than pK<sub>b</sub> (Bordbar-Khiabani & Gasik, 2022). As the surrounding pH changes, the charged groups of the hydrogels repulse one another. The water molecules and the ionized groups form hydrogen bonds, disintegrating the polymer network and increasing their hydrophilic nature. As the water enters the matrix due to a decrease in hydrophobic contact of the matrix, the hydrogel swells up (Deen & Loh, 2018). Hydrogels that incorporate methyl methacrylate or methacrylic acid show pH responsive behavior due to the presence of –COOH groups in their polymer chains with a pK<sub>a</sub> value of ~4. For healthy cells, the side groups are uncharged however, in diseased cells that have a pH greater than pK<sub>a</sub>, the polymer chains disintegrate to release the drug (Bordbar-Khiabani & Gasik, 2022). On the other hand, pK<sub>a</sub> higher than pH of the side group results in the protonation of the anion increasing the hydrophobic nature and shrinking the hydrogel. While the cationic hydrogel swells under these circumstances. Accordingly, accurate and effective drug release is dependent on the hydrogel polymer network be developed precisely. pH responsive hydrogels are also more stable mechanically and also have improved outcomes in oral delivery of the chemotherapeutic drug (Zhao et al., 2022).

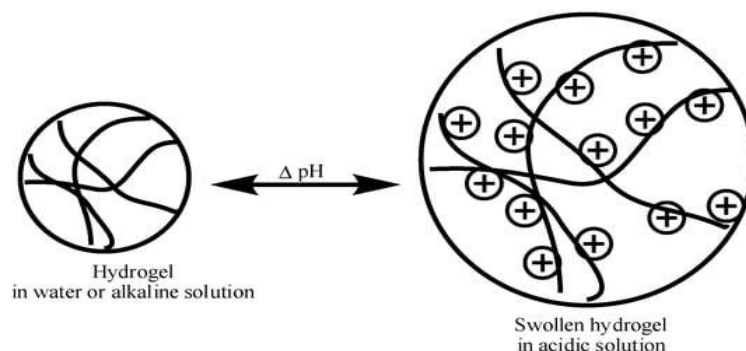


*Figure 2.1 pH dependant swelling of hydrogel matrix (Deen & Loh, 2018)*

In pH responsive monomers, acrylic acid is widely used in DDS. Monomers are selected according to the desired application keeping their pKa close to that of the tumor microenvironment for targeted drug release. A hydrogel system consisting of acrylic acid monomer in its backbone induces pH responsive behavior (Puranik, Pao, White, Peppas, & Biopharmaceutics, 2016). In a study, hydrogels sensitive to pH made of poly(methacrylic acid grafted ethylene glycol) showed modulated release into the intestine (Jacob et al., 2021). Hydrogels containing AA have been studied for swelling. Co-polymerization with gelatin, carboxymethyl cellulose (CMC), etc. has also been tested for different applications. The introduction of natural extracts like Aloe Vera (AV), echinacea, chamomile, etc. have shown enhanced activity as well (Bialik-Wąs, Pielichowski, & Biomaterials, 2018). pH responsive hydrogels have also been proposed for their improved swelling and release in acidic regions of the tumor microenvironment through the endocytic pathways (Dannert, Stokke, & Dias, 2019).

### *2.2.2. Crosslinking*

Structurally, polymers are the building blocks in hydrogels which can be synthetic, natural, or semisynthetic. These polymers can be hydrophobic or hydrophilic and the method of their crosslinking is the method of hydrogel preparation. Monomers, initiators, and cross linkers work together to form hydrogels (Ghasemiyeh & Mohammadi-Samani, 2019). Crosslinking of a hydrogel can be done physically or chemically. In physical crosslinking, hydrogen bonds are formed between monomers and it is reversible, while in chemical crosslinking, covalent bonds are formed and it is very much permanent. Physical crosslinking

does not require any crosslinking agent and can be done physically (Dattilo et al., 2023). Chemical crosslinking requires a free radical initiator, UV lamp/ gamma rays, or an electron beam. They can also be prepared thermally or by the addition of organic solvents, free-radical polymerization, enzymatic activity, etc. Improved stability is exhibited by such hydrogels due to enhanced mechanical and structural properties, and modifiable degradation patterns. On the other hand, since there is no chemical induction through initiators in physical crosslinking, drugs are less prone to degradation during hydrogel synthesis and it also offers reduced toxicity. The physical interactions also provide a scaffold for the efficient loading, encapsulation, and release of drugs (Jiang, Krishnan, Heo, Fang, & Zhang, 2020).

To attain optimized drug release kinetics, the right crosslinking mechanism and polymer type play a pivotal role. External factors like pH, temperature, environmental, and mechanical interactions also impact the desired traits in the hydrogel. It is also necessary to understand the electrostatic or chemical interactions between the matrix of the hydrogel and the drug for drug loading, degradation, and release. Thus, to achieve an optimized system, composition, crosslinking, and interactions need to be carefully designed, developed, and characterized (Chelu, Musuc, Popa, & Calderon Moreno, 2023).

### **2.3 The Tumor Microenvironment (TME) and Pathways Mutated**

The tumor microenvironment is a unique and dynamic mix of cancer cells surrounded by healthy supporting cells in the extracellular matrix. The healthy cells include adipocytes, fibroblasts, immune cells, etc. (Sepantafar et al., 2017). The cancer cells exhibit an abnormally high proliferation rate compared to the normal cells. These cells also have higher nutrient consumption power and faster metabolism, which the normal cells cannot compete with. The vasculature also grows and spreads extensively to provide nutrients to these cells (Khursheed et al., 2022). Several complex physical, chemical, and biological signals regulate cell proliferation. The tumor microenvironment provides the optimum conditions; extracellular matrix (ECM) stiffness, cytokines, growth factors, nutrients, oxygen, pH, etc., and also determines whether the cells can migrate and metastasize to distant parts (Park et al., 2017).

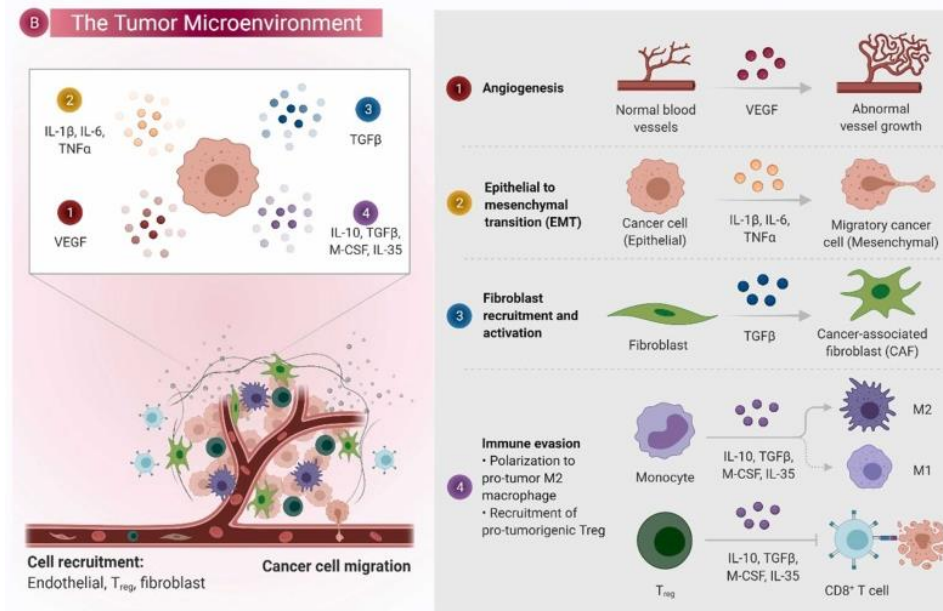
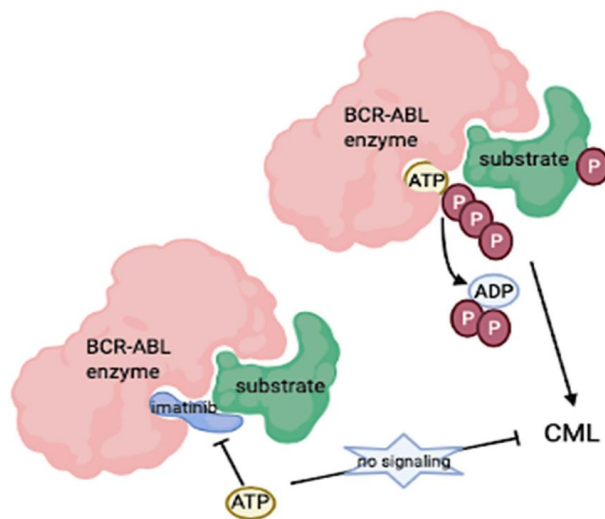


Figure 2.2 The tumor microenvironment and its associated factors involved in cancer progression (Khurshed et al., 2022)

## 2.4 Imatinib

Imatinib (IM), an anticancer agent, and an inhibitor of tyrosine kinase in the cell membrane suppresses cell proliferation by increasing apoptosis. Initially, IM was initially designed to treat patients who have the BCR-ABL mutation in the Philadelphia chromosome (Ph+), in chronic myeloid leukemia (Sobierajska et al., 2023). It is also one of the earliest targeted treatments used in cancer patients. IM works by inhibiting tyrosine kinase converting it into an inactivated state. It binds to the catalytic domain, the ATP pocket of the BCR-ABL1 protein, which is considered to be its vulnerable spot, and prevents the binding of ATP. Inhibition of the BCR-ABL1 protein reduces the proliferation and progression of cancer cells. This therapy is considered as ‘targeted therapy’ and has a different approach from the cytotoxic therapies, making it a lifelong therapy (Moschovi & Kelaidi, 2021). The goal of IM targeted therapy is to attain full hematological and a cytogenetic activity in 3-6 months, and at the molecular level 3 log reductions in 1 year. Even though this treatment is effective, some patients develop resistance at advanced stages. The mechanisms involved in the development are resistance are discussed under the next heading. Different strategies are under investigation for the reduction of drug resistance in IM (O'Dwyer, 2002). Additionally, the

ABCG2 transporter protein, which is also a drug resistance protein has also shown Involvement in inducing relapse and resistance among patients. The ABCG2 protein transports a number of chemotherapeutic agents like imatinib, methotrexate, gefitinib, etc. from the cells (Sogawa et al., 2021).



*Figure 2.3 demonstrates the mechanism of action of the anticancer agent; IM. The BCR-ABL kinase ATP binding region is occupied by IM which prevents phosphorylation, inhibiting the activity of the enzyme. CML; Chronic Myeloid Leukemia (O'Dwyer, 2002).*

## 2.5. Drug Resistance

The effectivity of chemotherapy is often compromised due to the low selectivity of the drugs and the efflux of the drugs out of the tumor cells by the P-glycoprotein (Pgp) present in their membranes. This causes cytotoxicity and drug resistance in the body (Ma et al., 2021). Traditional drugs, even though they have a good pharmacokinetic sketch, come with serious side effects, cytotoxicity, and even drug resistance. Acquired resistance has become one of the greatest problems in therapy. These issues increase the need for an efficient DDS that can delay the release of anticancer agents to prevent undesired side effects and cytotoxicity and reduce the chances of drug resistance. Hydrogels can prove to be valuable vehicles for the sustained release to the tumor microenvironment (Yang et al., 2018),(Pacheco et al., 2023). The basic mode of action for hydrogels and nanoformulations is to bypass the drug transporting molecules/proteins of the drug resistance pathways to combat this problem.

Delivering two or more drugs, inhibitors of efflux protein pumps, and pro-apoptotic molecules can also be achieved using hydrogels (Ma et al., 2021).

The mechanism of drug resistance in IM involves a mutation in the BCR-ABL genes and the amplification of its protein. Almost 90% of IM resistance accounts for this mutation. Additionally, increased concentrations of IM also increase in the multidrug resistance gene (MDR1) which encodes for the transporter Pgp in the membranes of tumor cells. As the concentration of Pgp increases, it depletes the intracellular IM by transporting it outside, acting as a pump, thereby reactivating the BCR-ABL signaling pathway. Alternatively, IM is also observed to be sequestered by the drug-binding proteins in the plasma initiating resistance. The alpha1 acid glycoprotein (AGP) is a plasma protein that binds to IM to inhibit its activity. The activation of substitute pathways inside the cells also results in IM resistance due to the loss of target dependence. This happens because the BCR-ABL pathway is also dependent on the activation of other tyrosine kinase pathways for disease progression like the Src family kinases that activate downstream of BCR-ABL (Burgess & Sawyers, 2006).

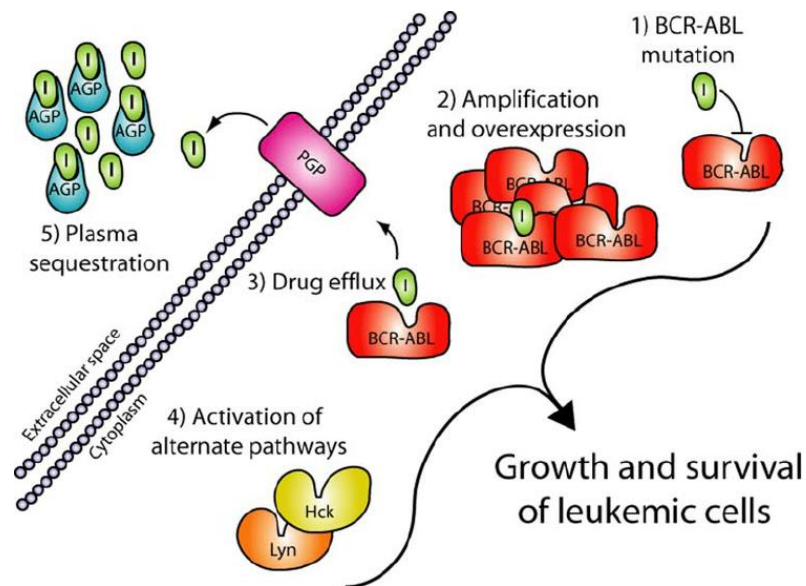


Figure 2.4 summarizes different mechanisms involved in resistance to IM in cancer cells. 1) Mutations in the BCR-ABL kinase domain prevents IM from binding. 2) Increased expression of the BCR-ABL also reduces the effect of IM resulting in resistance. 3) The expression of Pgp transporter proteins transports IM out of the cell. 4) Lyn and Hck are Src family kinases that act as alternate signaling pathways in cancer progression. 5) IM binding protein AGP binds to IM and inhibits its action (Burgess & Sawyers, 2006).



## 2.6 Aloe Vera

Aloe Vera (AV), belonging to the Liliaceae family, also known as *Aloe Barbadenesis* (Miller) is one of the most popular medicinal plants throughout the world. It is easily grown in people's homes. It is known far and wide for health and cosmetic benefits including; dietary supplements, herbal treatments, lotions, creams, face masks, ointments, medications for soothing skin during burns, psoriasis, eczema, wounds, and natural fertilizer, etc. The green fleshy leaves of the shrub plant are filled with a clear viscous gel containing a variety of bioactive compounds that act synergistically in their therapeutic activity. A single leaf of the aloe plant is divided into three layers: the outermost layer is a thick cortex covering the inner gel and produces the proteins and carbohydrates. The innermost layer is a gel comprising 99% water and 1% compounds including lipids, amino acids, sterols, polysaccharides, sugars, phenolic compounds, glucomannans, vitamins, etc. The yellow-coloured latex is present in the middle which is bitter and contains anthraquinones and glycosides. These compounds are collectively involved in providing health benefits like anti-tumor, anti-biotic, anti-oxidants, anti-ulcer, anti-diabetic, and anti-inflammatory properties which are important for diseases like gastrointestinal, cardiac, cancer, infectious wounds, skin diseases, and tissue regeneration, etc. Additionally, AV has an edge over other natural compounds due to its biocompatibility, biodegradability, tissue regeneration, bioavailability, moisturizing, and flexibility (Chelu et al., 2023).

Table 2.2 Compounds found in Aloe Vera and their advantages in biomedical applications (Chelu et al., 2023; Rahman, Carter, & Bhattarai, 2017)

Type	Compound	Function
Anthraquinones	Aloetic-acid, aloe-emodin, aloin, emodin, and isobarbaloin	Antiviral, anti-inflammatory, antioxidant, tissue regeneration
Carbohydrates	Mannan, glucomannan, acetylated mannan, acetylated glucomannan,	Important in pharmacological, medical, and industrial fields including various disorders, drug delivery systems, wound

	acemannan, cellulose etc.	treatment, etc.
Enzymes	carboxypeptidases, carboxylase, oxidase, alkaline phosphatase, amylase, lipase, superoxide dismutase, catalase etc.	Catalyze various biochemical reactions
Inorganic compounds	Calcium, chromium, chlorine, sodium, zinc, iron, potassium, phosphorus, copper, etc.	Aid in the enzyme activity in metabolic pathways
Amino acids	Alanine, glycine, histidine, lysine, aspartic acid, methionine, proline, etc.	Building blocks for proteins in the body and muscles
Proteins	Lectins	Hormones and anticancer activity
Saccharides	Mannose, aldopentose, glucose, L-rhamnose	Store and transfer energy, control cholesterol levels, metabolism and digestion, liver function, etc.
Vitamins	B-carotene, B1,2,6, C, choline, $\alpha$ -tocopherol, folic acid	Antioxidant effect by neutralizing free radicals
Miscellaneous	Triglycerides, cholesterol, steroids, lignins, salicylic acid etc	Promote wound healing

The anti-tumor activity of AV has been investigated in several cancers including; ovarian, adenocarcinomas, esophagus, breast, oral, colon, skin cancer, and squamous neoplasia and bone cancer, among many (Capes-Davis et al., 2010; Holliday & Speirs, 2011; Sánchez, González-Burgos, Iglesias, & Gómez-Serranillos, 2020). A study on liver HepG2 cancer cells demonstrated that AV and *Calligonum Comosum* extracts cause cytotoxicity and genotoxicity in the cells by inducing apoptosis and DNA damage. Cell viability was investigated through the MTT assay (Kudłacik-Kramarczyk et al., 2021). The immunomodulatory activity was assessed which showed a reduction in IL-8, 6, 1 $\beta$ , and TNF- $\alpha$  cytokine production exhibiting anti-inflammatory effects (Ashouri et al., 2019). While enhanced production of interferon and tumor necrosis factor IL-1, AV exhibited tumor necrosis and tumor shrinking. Alternatively, the mannose receptors are enhanced in the tumor associated macrophages and expressed significantly in tumor cells. Resultantly, attracting the mannose and acemannan polymers toward the tumor cells and delivering drugs to them (Sadgrove & Simmonds, 2021). In another study AV extracts of different concentrations resulted in cancer cell cytotoxicity in HeLa and MCF-7 cell lines. Apoptosis and genotoxicity were induced (Hussain, Sharma, Khan, Shah, & Haque, 2015). Aloe-emodin has also resulted in apoptosis by inhibiting oxidative stress in mitochondrial and endoplasmic reticulum in the same cell lines (Sánchez et al., 2020). Emodin, a compound of AV has also exhibited BCL-2 levels suppression and cell proliferation and a surge in caspase 3 and Bax in mucosa cancer cell lines (Liu et al., 2018). In esophagus cancer, aloe-emodin suppresses AKT and ERK phosphorylation reducing cell proliferation (Chang et al., 2016). Activation of apoptosis, and increase in intracellular calcium and ROS production has also been identified in cancer cells (Chen et al., 2018; Sánchez et al., 2020).

### *2.6.1. Aloe Vera Hydrogels*

AV is a natural and biocompatible polymer used in making hydrogels. The AV gel can be extracted from mature AV leaves. The leaves are cut, washed and the yellow latex layer is removed, and washed again with water or ethanol to get rid of any impurities. The formulation can be mixed with the appropriate concentration of polymers and crosslinking agents to form the final shape. The hydrogel is then rinsed to eliminate any excess of unreacted agents and stored in a cold setting.

Several mechanisms can be used for cross-linking of AV hydrogels; in chemical cross-linking, an initiator is used as a cross-linker to form covalent bonds with OH groups in AV. In physical cross-linking, pH and temperature variations can be used to form the hydrogel. Divalent cations like calcium chloride (CaCl<sub>2</sub>) are usually used as a cross linker to alginate-AV hydrogels. The CaCl<sub>2</sub> reacts with the alginate to form the gel. In temperature induced gelation, physical crosslinking occurs when the temperature is increased above a set point. In chemical crosslinking, compounds like genipin, tannic acid, glutaraldehyde, etc are used to cross gels. Ionizing radiations like UV, gamma rays, or electron beams can also be used in chemical cross-linking by inducing free radical polymerization. The hydrogel is washed after cross-linking to remove any unreacted and undesired agents.

The right crosslinking mechanism is crucial to achieve swelling properties, biocompatibility, degradation, mechanical stability, drug loading, and release. A number of parameters like pH, temperature, and release kinetics can be regulated by using the right cross-linker. The drug is loaded into the gel before cross-linking either by dissolving the gel in a solvent or by incorporating it in the gel solution. The selection of the drug depends on the desired therapeutic effect of the gel. The loaded AV hydrogel is then characterized for its structural and functional groups, its physical, biological, and chemical composition can be analyzed by investigating the swelling behavior, gel fraction, mechanical properties, and drug release, and the biochemical activity can be assessed by in vitro, and in-vivo analysis (Chelu et al., 2023).

### *2.6.2 Properties of Aloe Vera Hydrogels*

AV has great significance in medical applications where it is most frequently used to enhance the water absorbability of drugs that's are poorly absorbed by the system. It has the ability to encapsulate these drugs and deliver them acting as a stabilizing agent. As a result, these advantages of AV can be further explored to expand its applications in DDS. The following mechanisms aid in drug release from the AV hydrogel:

*Diffusion based release:* Diffusion is one of the most fundamental mechanisms working inside the body. The drug is released from the hydrogel matrix based on the difference in hydrogel and environment gradient inside the body. In such a mechanism, the pore size and

pore uniformity of the hydrogel matrix influence the release kinetics from the hydrogel system (Chelu et al., 2023).

*Swelling based release:* AV, in general, can absorb 90% water from its surroundings. The AV hydrogel absorbs water and swells up when exposed to an aqueous medium, releasing the encapsulated drug. The swelling behavior expands the matrix, which creates pores inside the gel assisting in the release. Hydrogel composition, crosslinking, and the environment influence the swelling behavior (Chelu et al., 2023).

*Degradation based release:* AV acts as a biodegradable agent inside the body. It can endure a controlled rate of degradation releasing the drug from its matrix. Various factors, like enzymes, hydrolysis, chemicals, or environmental conditions can lead to hydrogel degradation (Chelu et al., 2023).

*Localized drug release:* AV hydrogels offer localized drug release to targeted sites. It can deliver both hydrophobic and hydrophilic drugs, different proteins, and small biomolecules inside the tumor microenvironment (Ketabat et al., 2019).

## **2.7. Scope of the Study:**

The current study/research is limited to the synthesis of Aloe Vera hydrogels, their characterizations, physiochemical analysis followed by biochemical and in-vitro analysis.

## CHAPTER 3: MATERIALS AND METHODOLOGY

### 3.1 Materials

This section enlists all the equipment, reagents, media, and materials used in the research work to produce this thesis

#### 3.1.1 Equipment

Table 3.1 List of equipment used during the study and their manufacturers

<i>Equipment</i>	<i>Manufacturer</i>
<i>SEM</i>	Joel JSM-6490A
<i>Hot Plate</i>	SCIOLOGEX MS-H280-Pro
<i>Laminar Flow Cabinet</i>	ISOCIDE
<i>Centrifuge</i>	HERMLE Z206 A
<i>Incubator</i>	WiseCube
<i>UV-Vis spectrophotometer</i>	BMS UV-2800
<i>Laboratory Oven</i>	WiseVen
<i>Weighing balance</i>	RADWAG PS360//C/1

### 3.1.2 Reagents/Chemicals

Table 3.2 List of chemicals used in the study and their manufacturers

<i>Chemicals</i>	<i>Manufacturer</i>
<i>Sodium Alginate</i>	Sigma Aldrich
<i>Poly Vinyl Alcohol</i>	Sigma Aldrich
<i>Acrylic Acid</i>	Sigma Aldrich
<i>Gelatine</i>	SolarBio
<i>IM</i>	Macklin
<i>Calcium Chloride</i>	Sigma Aldrich
<i>PBS</i>	Sigma Aldrich
<i>Ethanol</i>	Sigma Aldrich
<i>MTT</i>	Sigma Aldrich
<i>Fetal Bovine Serum (FBS)</i>	Sigma Aldrich
<i>DMEM</i>	Sigma Aldrich/ Solar Bio
<i>DMSO</i>	Sigma Aldrich

### 3.1.3 Solutions Used for Hydrogel Synthesis

Table 3.3 Solutions Prepared for Hydrogel Synthesis

<i>S no.</i>	Components	g/100ml
1	SA	2
2	PVA	10
3	AV	20
4	Gelatine	1
5	AA	1
6	CaCl <sub>2</sub>	5

### 3.1.4 Solutions used for swelling, degradation, and release profiling

Table 3.4 Solutions Prepared for Physiochemical Analysis

<i>S no.</i>	Components	Quantity (1pc/100ml)
1	PBS Tablet	1
2	Distilled water	100



### 3.1.5 Solutions used for cell culture

Table 3.5 Solutions prepared for cell culture viability activity

<i>S no.</i>	Components	Quantity
1	MTT	5mg/ml
2	IM	25µg/ml
3	FBS	50µl/ml
4	DMSO	1µl/ml
5	PBS	1/100ml

## 3.2. Methodology

### 3.2.1 Aloe Vera gel extraction

The AV gel was extracted by the procedure discussed by (Chelu et al., 2023) and (Kenawy et al., 2023).

#### 3.2.1.1 Step 1: Collection of AV Leaves

Fresh and healthy AV leaves 30-50cm were cut and collected from a 3 to 5 year old AV plant grown in a local garden in Pakistan.

#### 3.2.1.2 Step 2: Washing and Disinfecting

DI water was used to rewash the AV leaves followed by an ethanol rinse at room temperature to remove any impurities. The leaves were clipped transversally and the yellow latex layer was removed by washing again with distilled water.

### *3.2.1.3 Step 3: Extraction of Inner Gel*

Spikes from the margins were removed and the parenchyma was separated. The exposed epidermis/inner gel was rewashed and extracted using a spoon.

### *3.2.1.4 Step 4: Homogenization of the Gel and Centrifugation*

The inner gel was then homogenized in a blender followed by centrifugation at 3000 rpm for 30 min at 4° C to remove fibres.

### *3.2.1.5 Step 5: Obtaining Fresh AV extract*

The separated supernatant was collected and sieved through Whatman filter paper to get fresh AV extract. The freshly prepared AV extract was then stored at -20 C until further use (Chelu et al., 2023; Kenawy et al., 2023). This AV gel extract serves as a biocompatible polymer to form the hydrogel by mixing it with suitable copolymers and a crosslinking agent.

## *3.2.2 Synthesis of hydrogel*

The AV hydrogels were synthesized according to the procedure followed by (Bialik-Wąs, Królicka, & Malina, 2021).

### *3.2.2.1 Formation of Solutions*

To synthesize the PVA/SA/AV hydrogels, solutions of PVA (10% w/v), SA (2% w/v), gelatine (1% w/v), CaCl<sub>2</sub> (5% w/v), and 20% AV were prepared in autoclaved distilled water, by mixing in a magnetic stirrer, under appropriate temperature conditions. 1% AA solution was also prepared in distilled water.

### *3.2.2.2 Mixing Step*

SA, PVA, and AV solutions were mixed using a magnetic stirrer at 80° C, by calculating the required amount. 1% AA was added to set the pKa at 4 and induce pH responsive behavior of the hydrogel. 25 µM IM was also added in the drug loaded hydrogel during the mixing step.

Table 3.6 Hydrogel Composition

<b>Gels</b>	<b>SA (%)</b>	<b>PVA (%)</b>	<b>AV (%)</b>	<b>AA (%)</b>	<b>IM (<math>\mu</math>M)</b>
<b>PVA/SA</b>	2	10	0	1	0
<b>PVA/SA/AV</b>	2	10	20	1	0
<b>PVA/SA Drug</b>	2	10	0	1	25
<b>PVA/SA/AV Drug</b>	2	10	20	1	25

### 3.2.2.3 Polymerization, Casting and Crosslinking

The hydrogel solution was kept at 80° C for 1.5 h for polymerization of the incorporated polymers. The solutions were left at room temperature for 24 h for casting. The following day, the sample was added in 5% CaCl<sub>2</sub> solution to form the hydrogels.

### 3.2.2.4 Washing of the Gels

Finally, the gels are washed in PBS to remove unreacted CaCl<sub>2</sub> to avoid immoderate crosslinking. Freshly prepared hydrogels were then used for characterization and further in-vitro analysis

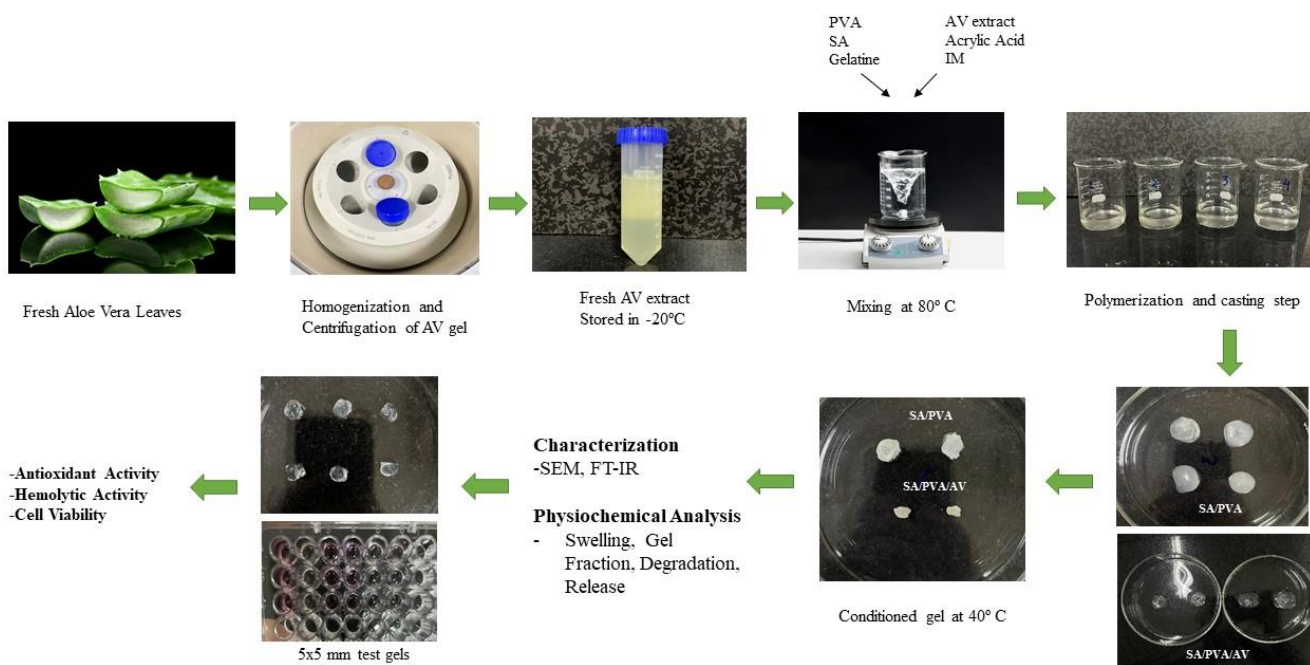


Figure 3.1 Steps in the extraction of AV gel and the formation of AV hydrogel

### 3.2.3 Characterizations

#### 3.2.3.1 FTIR

The hydrogels were conditioned for 24 h at 40° C in a lab oven and ground in a pestle and mortar to form a fine powder. The powdered samples, about 1-2 mg were then mixed with spectroscopic grade KBr about 200mg (1:100), and ground to obtain a homogenous mixture which was transferred to a pallet die. A hydraulic press was used to apply pressure. A transparent pallet was obtained, which was placed on the pallet holder in the spectrometer. The chemical structure and functional groups were analyzed using the infrared FT-IR spectrometer in the range 4000-400  $\text{cm}^{-1}$  at 20 spectral scans with a resolution of 2  $\text{cm}^{-1}$ .

#### 3.2.3.2 SEM

The morphology in  $\mu\text{m}$  and  $\text{nm}$  was observed using the Scanning Electron Microscopy (SEM) which produces optical representation in high resolution from their surface and cross-section. The synthesized AV hydrogel groups were conditioned for 24 h at 40° C in a lab oven until completely dried. The gels were then cut into half to obtain their cross-section. The

samples were then attached to a conductive stub using a conductive tape. A conductive thin gold (Au) layer was deposited onto the dried AV hydrogel through sputtering. The stub was then mounted inside the SEM and images were taken at an acceleration voltage of 5.0 kV at different magnifications.

### *3.2.4 Physiochemical Analysis*

#### *3.2.4.1 Swelling Analysis*

The swelling behavior of the hydrogels was determined by drying the gels in a laboratory oven and then soaking them in PBS solution. The hydrogels were cut into 1 x 1 cm<sup>2</sup> circles and then conditioned at 40° C in a dry oven overnight. The initial weight was recorded by weighing the dried hydrogels. The hydrogels were then immersed in PBS solutions with pH 6.4 and pH 7.4 at room temperature. Final weight (Wf) recordings were then taken at 5 min, 15 min, 30 min, 1h, 6hr, and 24 h after removing the excess solution with tissue paper. The percentage swelling was determined through the following Eq. 1

$$\text{Swelling (\%)} = \left( \frac{W_f - W_i}{W_i} \right) * 100 \quad \text{Eq. 1}$$

Wi= initial dry weight of the hydrogel, Wf = final swollen weight of the hydrogel (Nazir et al., 2021)

All samples were taken in triplicates

#### *3.2.4.2 Gel Fraction*

To determine the gel fraction, the 1 x 1 cm<sup>2</sup> fresh samples were dried and their initial weight (Wi) was taken. The samples were then soaked at room temperature in PBS solution with pH 6.4 and pH 7.4 for 24h. The swollen hydrogels were reconditioned at 40° C for 24 h and weighed again (Wf). The percentage of gel fraction was determined through Eq. 2 (Afshar et al., 2020)

$$\text{Gel Fraction (\%)} = \left( \frac{W_f}{W_i} \right) * 100 \quad \text{Eq. 2}$$

All samples were taken in triplicates

#### 3.2.4.3 Degradation

To determine the in vitro biodegradation behavior of the hydrogels, the respective gels were cut into 1 x 1 cm<sup>2</sup> circles, conditioned at 40° C for 24 h, and weighed. The hydrogels were immersed in 5 ml PBS solution with pH 6.4 and pH 7.4 and placed in an incubator at 37° C under 5% CO<sub>2</sub>, standard body conditions to observe degradation over time. Final weights were recorded at different time intervals 24h, 48h, 72h, and 144h. The samples were reconditioned under the same conditions as before. The biodegradation percentage was determined using Eq. 3 (Kenawy et al., 2023; Nazir et al., 2021).

$$\text{Degradation (\%)} = \left( \frac{W_f - W_i}{W_i} \right) * 100 \quad \text{Eq. 3}$$

Where, W<sub>i</sub>= initial weight of the hydrogel, W<sub>f</sub>= final weight of the hydrogel at different intervals

All samples were taken in triplicates

#### 3.2.4.4 Encapsulation Efficiency of AV Hydrogel

The efficiency of IM encapsulation in the AV hydrogel was determined by slightly modifying Dadashzadeh, et al.'s (Dadashzadeh, Imani, Moghassemi, Omidfar, & Abolfathi, 2020) protocol. The prepared hydrogels were immersed in PBS solution, vortexed, and centrifuged at 13,000 rpm at 4° C for 30 min to extract their constituents. The supernatant was filtered and collected. The absorbance of the supernatant was measured at 260nm, similar to that of IM. EE was calculated using the formula Eq. 4

$$\text{Encapsulation Efficiency (\%)} = \left( \frac{W_t - W_i}{W_t} \right) * 100 \quad \text{Eq. 4}$$

Where W<sub>t</sub> is the quantity of loaded IM in the suspension and W<sub>i</sub> is the free IM

#### 3.2.4.5 Drug Release

The release behavior of IM from the hydrogels was assessed by soaking 1 x 1 cm<sup>2</sup> hydrogels in 5 ml PBS with pH 6.4 and pH 7.4 at 37° C and 100 rpm in a shaking incubator. The sample solution was drawn at different intervals; 0 min, 10 min, 30 min, 60 min, 6 h, and

24 h. The solution was replaced by fresh PBS to maintain the volume. The concentration of the solutions was then determined through the ultra-violet (UV-Vis) spectrophotometer at 260 nm based on the standard curve lambda max. The absorbance curve was calculated by using different concentrations of IM (0 to 30 µM) at room temperature. The percentage of drug released at each time point was calculated by the difference of total drug release to the initial amount of loaded drug Eq. 5 (Sobierajska et al., 2023)

$$\text{Drug Release (\%)} = \left( \frac{W_f - W_i}{W_i} \right) * 100 \quad \text{Eq. 5}$$

### 3.2.5 Antioxidant Activity

The scavenging activity of the hydrogels was investigated by performing the 2,2-diphenyl-1-picrylhydrazyl radical (DPPH) assay (Ishfaq, Khan, Khalid, & Asghar, 2023). 0.1 mM solution of ethanolic DPPH was prepared and vortexed for complete dissolution. The hydrogels were cut into 5x5mm size and weighed. These gels were added into 2.5 ml of DPPH solution and incubated for 1 h in the dark to allow radical scavenging activity. The readings were recorded at 517 nm and the absorbance (%) was calculated using Eq. 6

$$\text{Scavenging Activity (\%)} = \left( \frac{\text{Abs blank} - \text{Abs sample}}{\text{Abs blank}} \right) * 100 \quad \text{Eq. 6}$$

### 3.2.6 Biocompatibility

To investigate the in-vitro biocompatibility of the PVA/SA/AV hydrogels, a hemolysis assay was carried out using an Institutional Human Ethical Committee of Chettinad Academy of Research and Education's approved protocol followed by (Bhoopathy et al., 2024). Fresh blood from healthy subjects was withdrawn and its components were isolated by centrifuging at 3000 rpm for 5 min. The supernatant containing the plasma and buffy coat was eliminated followed by washing of the pallet and centrifuging thrice until clear supernatant was achieved to obtain the RBCs. A 1% RBC solution was made in PBS. PVA/SA and PVA/SA/AV hydrogels were cut into 1 x 1 cm<sup>2</sup> and incubated in PBS solution. The hydrogels were then incubated with 50 µl RBCs at 37° C for 60 min. RBCs incubated in DI water were taken as positive control and RBCs incubated in PBS were taken as negative control. The incubated samples for were centrifuged finally at 3500 rpm for 10 min and the supernatant was collected

to record absorbance at 540 nm using UV-spectrophotometer. The percentage (%) of hemolysis was determined using Eq.7

$$\text{Hemolysis (\%)} = \left( \frac{\text{Sample Abs} - \text{Control Neg}}{\text{Control Pos} - \text{Control Neg}} \right) * 100 \quad \text{Eq. 7}$$

All samples were taken in triplicates.

### 3.2.7 Cell viability

An MTT assay was performed to evaluate the cytotoxic levels of the hydrogels. The MCF-7 breast cancer cell lines were obtained from Dr. Aneela Javed, (Atta-Ur-Rahman School of Applied Bio-Sciences (ASAB), NUST, Islamabad, Pakistan).

#### 3.2.7.1 Cell Thawing and Passaging

Cryopreserved cells were thawed rapidly in a water bath at 37° C. DMEM medium was prepared by supplementing with 10% FBS and 1% penicillin-streptomycin. The cells were then transferred into cell culture flasks, containing the supplemented DMEM, pre-warmed and incubated at 37° C and 5% CO<sub>2</sub>. As the cells reached 80-90% confluency, the old medium was aspirated and washed with PBS. The cells were detached by adding trypsin-EDTA and then neutralized using the supplemented medium. The cells were then centrifuged at 1000 rpm for 5 min and resuspended using supplemented medium

#### 3.2.7.2 Cell Counting

A cell suspension was made by trypsinized cells, 10µl and trypan blue, 10µl was added which acts as a staining dye. The cells were then loaded in a hemocytometer to determine their viability. Cell concentration was counted using the formula, Eq. 8

$$\text{Cell Conc.} \left( \frac{\text{cells}}{\text{ml}} \right) = \text{avg no. of cells per square} * \text{dilution factor} * 10^4 \quad \text{Eq. 8}$$



### 3.2.7.3 Cell Plating

The cancer cells were seeded at the concentrations of 10,000 cells per well in the 96 well plates. The culture plates were allowed to adhere by incubating at 37° C, 5% CO<sub>2</sub>, and 95% humidity. The next day, the supernatant was supplemented by 5% FBS.

### 3.2.7.4 Treatment

Hydrogels of 5 x 5 mm were cut according to the well size of the 96 well plate and were added. The hydrogels were loaded with 25 µM of IM, prepared in 0.1% DMSO.

### 3.2.7.5 MTT Assay

The cultures were washed after 72h. MTT ((3- (4,5-dimethylthiazol-2- yl)-2) reagent (10 mg/ml) prepared in PBS solution was added and incubated for 2 h. The supernatant was replaced and DMSO was added to dissolve the purple MTT crystals. The culture was shaken for 30 min, later the absorbance was determined using the microplate reader at 570 nm (Sobierajska et al., 2023). The cell viability percentage was calculated using the Eq. 9

$$\text{Cell viability (\%)} = \left( \frac{\text{Sample abs} - \text{Blank abs}}{\text{Control abs} - \text{Blank abs}} \right) * 100 \quad \text{Eq. 9}$$

All tests were performed in triplicates

### 3.2.7 Statistical Analysis

All of the obtained data were analyzed statistically using GraphPad Prism 10. After checking the normality of the data, one-way analysis of variance (ANOVA) was applied to determine the difference of means among the tested groups. Graphs were made using OriginPro and GraphPad Prism software. A value of P < 0.05 was considered statistically significant.

## CHAPTER 4: RESULTS

### 4.1 Characterization

#### 4.1.1 FT-IR

The hydrogels were observed for their characteristic functional groups through FT-IR analysis Fig. 4.1. PVA/SA hydrogels and PVA/SA/AV hydrogels unloaded and loaded with IM were compared. The presence of AV in the gels did not affect the chemical structure to a greater extent as shown in the spectra. A wide range of bands present from 3000-3500  $\text{cm}^{-1}$  in the spectra represents the  $-\text{OH}$  stretching vibrations of SA, PVA, AV, and its active substances like carboxylic groups, alcohols, phenols, etc. The bands are slightly more intensive in AV hydrogels due to stronger H-bonds and polysaccharides present. The intense peak at 3250  $\text{cm}^{-1}$  in the PVA/SA IM loaded and PVA/SA/AV IM loaded hydrogels correspond to the  $-\text{NH}$  stretching peak of IM. The intensity of the peak confirms the bonding of IM with the  $-\text{OH}$  and H bonds of SA, PVA, and AV. The vibrational peak at 2930  $\text{cm}^{-1}$  represents the CH stretching of PVA, SA, and AV. The peak at 1035  $\text{cm}^{-1}$  represents the CO and C-OH bonds of glucan in polysaccharides of AV and SA. The range from 1540-1650  $\text{cm}^{-1}$  corresponds to the stretching of C=C and C-C, C-N of pyrimidines and aminopyrimidines of PVA and IM, respectively, where broadened 1648  $\text{cm}^{-1}$  is equivalent to the C=O stretching of amide in hydrogels loaded with IM. This confirms the presence of IM in the hydrogels. Peaks around 1036  $\text{cm}^{-1}$  represent C-O of IM and C-O=C glycosidic bonds of AV. The peak at 820  $\text{cm}^{-1}$  shows out of plane bending of the group, C-H.

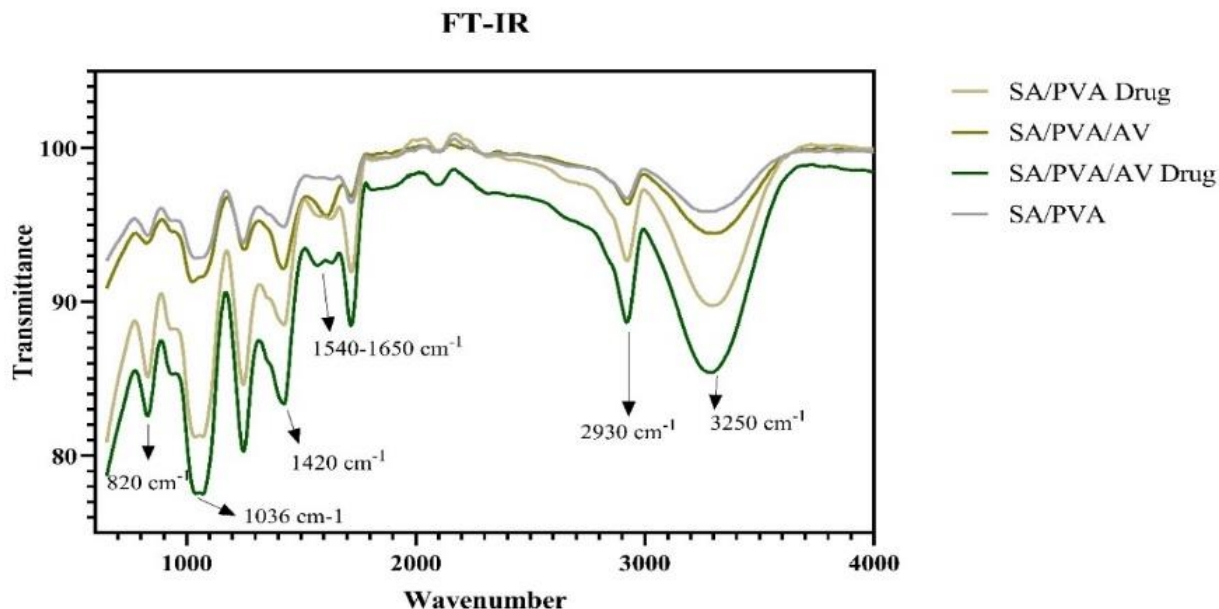


*Figure 4.1 FT-IR spectra of PVA/SA and PVA/SA/AV loaded and unloaded hydrogels with IM*

#### 4.1.2 SEM

The SEM analysis of the unloaded and loaded PVA/SA/AV hydrogels with IM is shown below in Fig. 4.2. The surface morphology, as well as the cross sections were observed which exhibited notable differences. The surface of the unloaded hydrogel is somewhat rough with small and irregularly sized micro and nanopores scattered, while the IM loaded hydrogel showed an evident change in morphology, with larger pore size and more irregular distribution confirming the incorporation of IM into the hydrogel. The cross-section of the gels shows a porous 3D structural morphology with multiple layers of internal matrix. The PVA/SA/AV unloaded hydrogel exhibited an irregular structure and smaller sized pores, while the loaded PVA/SA/AV hydrogel showed a more regular porous structure which could be due to the efficient crosslinking of IM with the hydrogel AV and PVA matrix.

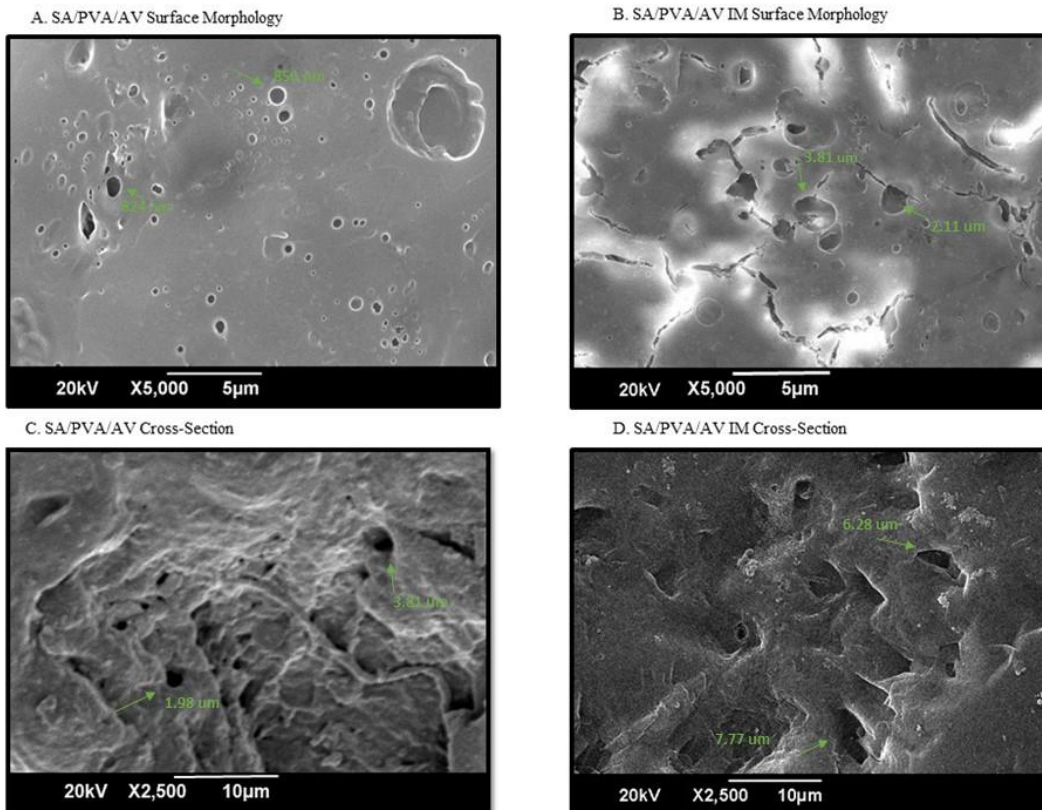


Figure 4.2 SEM Images of A) surface morphology of PVA/SA/AV unloaded hydrogels, B) surface morphology of PVA/SA/AV hydrogels loaded with IM.

#### 4.1.3 Elemental Analysis:

The elemental composition of the hydrogels was confirmed through the Energy Dispersive X-ray (EDX) analysis. The appearance of Oxygen (O) and Carbon (C) on the surface of the hydrogel indicated the presence of PVA and AV. The presence of Calcium ( $\text{Ca}^{+2}$ ) can be associated with the residues of unreacted cross-linker  $\text{CaCl}_2$  on the sample surface. In the IM loaded PVA/SA/AV hydrogel, the element nitrogen (N) confirms the presence of IM, Fig. 4.3.

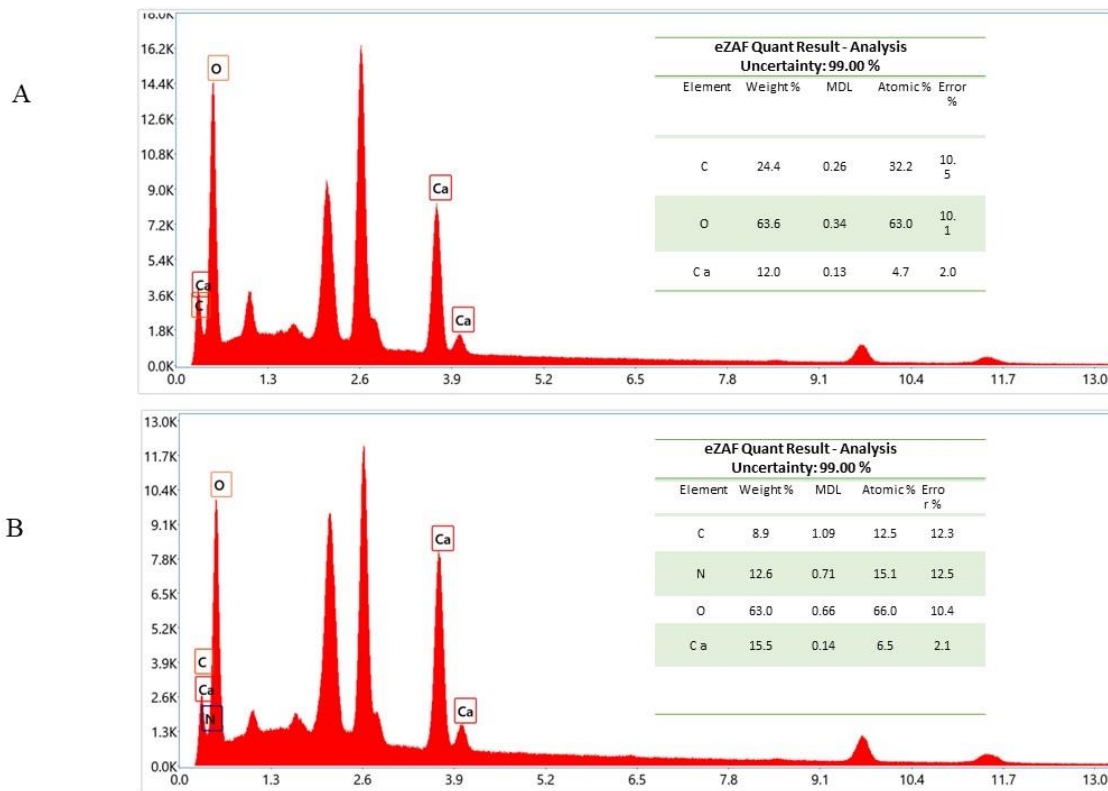


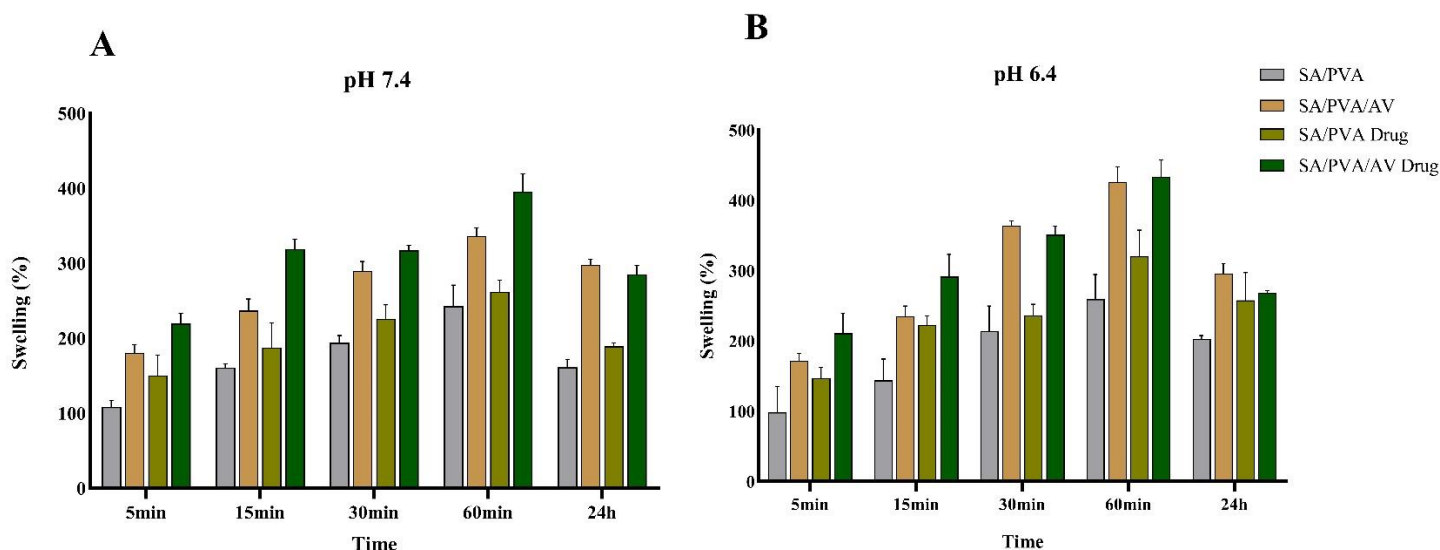
Figure 4.3 EDX of A) PVA/SA/AV unloaded hydrogels, B) PVA/SA/AV hydrogels loaded with IM

## 4.2 Physiochemical Analysis

### 4.2.1 Swelling Analysis

The water absorption ability of the loaded and unloaded hydrogels was investigated by immersing the dried hydrogels in PBS solution at pH 7.4 (blood pH) and pH 6.4 (tumor cell pH) at room temperature, Fig. 4.4. The soaked hydrogels were paper dried to remove any excess PBS solution before weighing. A noteworthy increase in the weight of hydrogels, 107%, 150% for PVA/SA unloaded and IM loaded hydrogels and 180%, 210% for PVA/SA/AV unloaded and loaded hydrogels within 5 minutes in pH 7.4 while the pH 6.4 hydrogels also exhibited a similar pattern with 100%, 140%, increase in PVA/SA unloaded and IM loaded hydrogels and a 170% and 210% increase in PVA/SA/AV unloaded and loaded hydrogels, was seen. After 1h of immersion, the hydrogels in pH 6.4 exhibited a dramatically increased rate of swelling at 260%, 320% for PVA/SA unloaded and loaded hydrogels and 420%, 430% for PVA/SA/AV unloaded and loaded hydrogels, compared to

240%, 260%, 330%, and 390% increase in PVA/SA loaded and unloaded and PVA/SA/AV loaded and unloaded hydrogels respectively. As the hydrogels reached equilibrium swelling, their percentage weights decreased after 24h of immersion. Hydrogels immersed in pH 6.4 exhibited a more sustained and higher swelling rate compared to pH 7.4, while the PVA/SA/AV hydrogels exhibited better swelling properties compared to PVA/SA hydrogels confirming that the incorporation of AV enhances the water absorbability due to its hydrophilic nature and by introducing an amorphous porous structure into the gels. IM loaded hydrogels showed more swelling compared to unloaded hydrogels due to the enlarged pore sizes after the incorporation of IM.



**Swelling Analysis**

C.

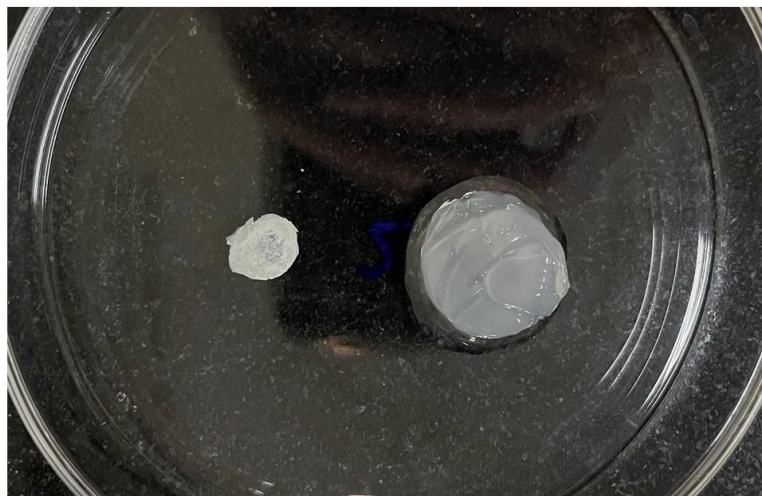


*Figure 4.4 Swelling Analysis of A) PVA/SA and PVA/SA/AV unloaded and loaded hydrogels with IM at pH 7.4, B) PVA/SA and PVA/SA/AV unloaded and loaded hydrogels with IM at pH 6.4, C) Pictorial Representation of dried and swollen hydrogel*

#### *4.2.2 Gel Fraction*

The intensity cross-linking was analyzed by determining the gel fraction percentage. The results show that the hydrogels with higher PVA and SA content showed higher gel fraction percentages while the hydrogels with AV content showed lower levels of cross-linking, Fig. 4.5.

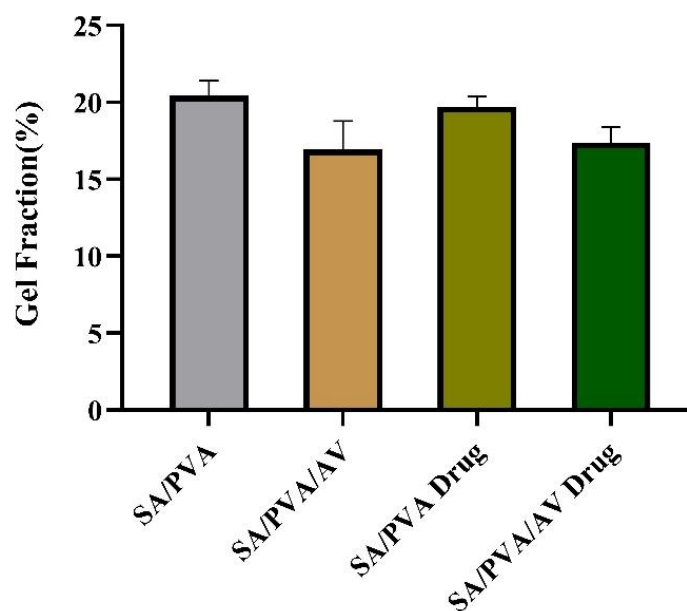


*Figure 4.5 Gel fraction of PVA/SA and PVA/SA/AV unloaded and loaded hydrogels with IM*

#### *4.2.3 In-vitro Degradation*

The in-vitro degradation behavior of the PVA/SA and PVA/SA/AV unloaded and loaded hydrogels was investigated at two pH ranges, pH 7.4 for blood, and pH 6.4 for tumor cells, as shown in Fig. 4.6. The gels were immersed in PBS solutions as a function of time for up to 144h under standard incubation. At both pH 7.4 and pH 6.4, a general trend was observed. The PVA/SA loaded and unloaded hydrogels showed around 50% degradation after 24h of immersion while the PVA/SA/AV hydrogels showed a considerable rate of degradation at around 70% and 80% unloaded and loaded after 24h. At pH 7.4, after 144h, the PVA/SA and PVA/SA/AV unloaded and loaded hydrogels exhibited a similar rate and all were degraded up to 90% respectively. At pH 6.4, the PVA/SA unloaded and loaded hydrogels demonstrated degradation of around 88% while the PVA/SA/AV unloaded and loaded hydrogels were dramatically degraded by around 100%. This confirms that the presence of AV has enhanced the degradability of the hydrogels.



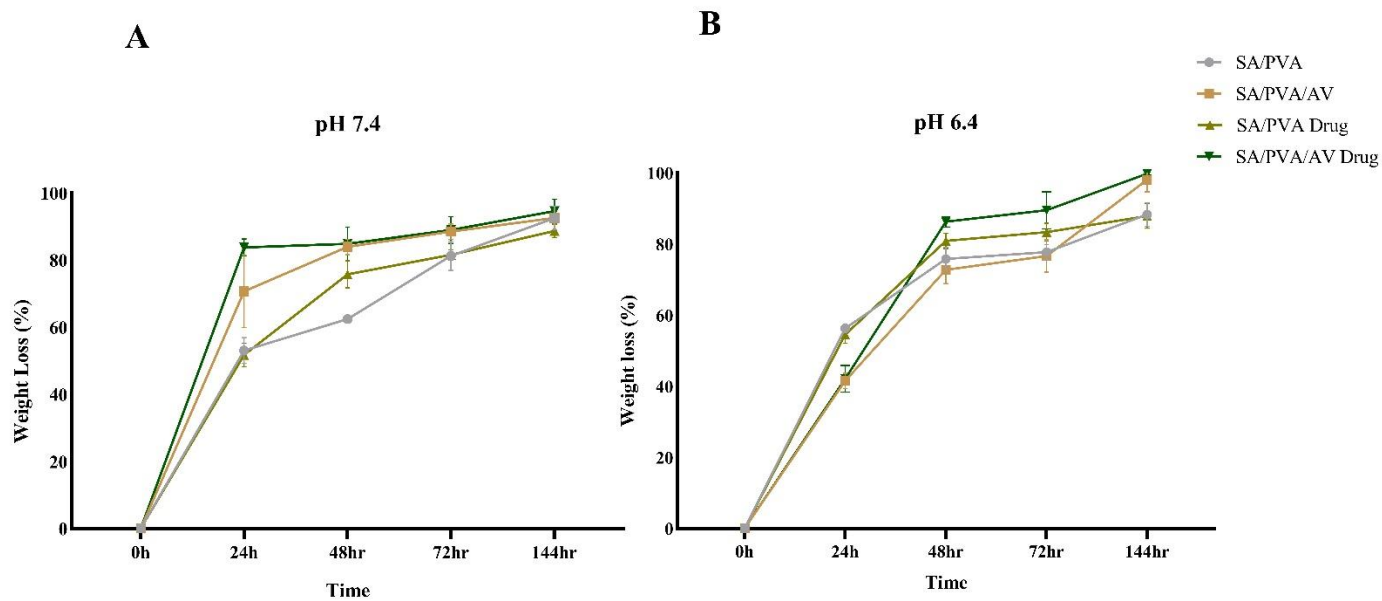


Figure 4.6 Degradation Analysis of A) PVA/SA and PVA/SA/AV unloaded and loaded hydrogels with IM at pH 7.4, B) PVA/SA and PVA/SA/AV unloaded and loaded hydrogels with IM at pH 6.4

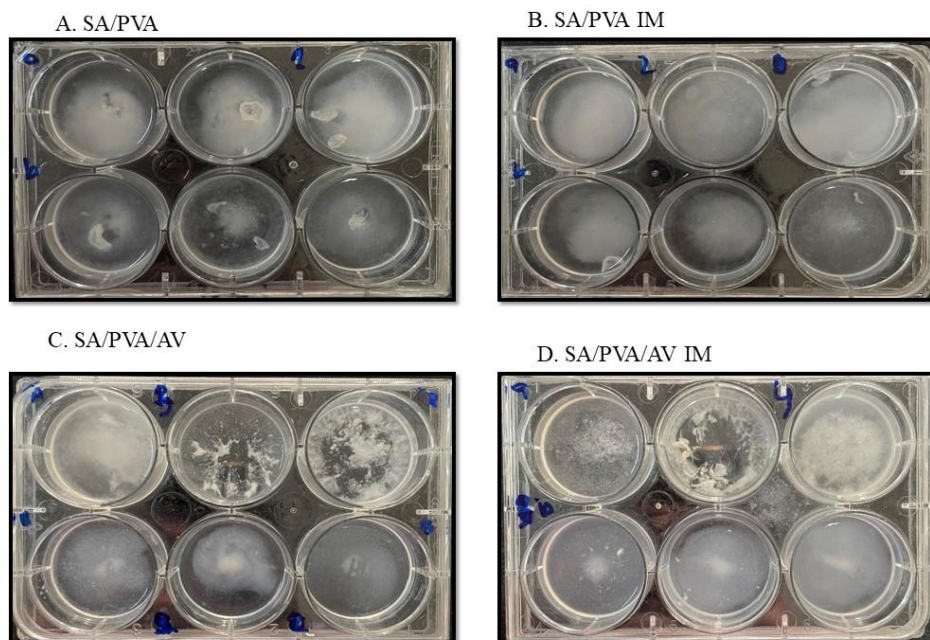


Figure 4.7 Pictorial Representation of A) PVA/SA, B) PVA/SA IM, C) PVA/SA/AV, D) PVA/SA/AV IM hydrogels after 144 h of degradation period.

#### 4.2.4 Encapsulation Efficiency of AV Hydrogel

The calculated efficiency of the IM encapsulated PVA/SA and PVA/SA/AV hydrogels in triplicates is demonstrated in the table below. The PVA/SA hydrogels exhibited somewhat similar EE (%) compared to PVA/SA/AV hydrogels, with no noteworthy differences.

Table 4.1 IM encapsulation efficiency of PVA/SA and PVA/SA/AV loaded hydrogels with IM in triplicates

<b>S no.</b>	<b>Free IM (abs)</b>	<b>PVA/SA Drug (abs)</b>	<b>PVA/SA/AV Drug (abs)</b>	<b>EE (%) PVA/SA Drug</b>	<b>EE (%) PVA/SA/AV Drug</b>
	0.149	0.344	0.371	56	59
	0.146	0.353	0.349	58	58
	0.158	0.349	0.376	54	58

#### 4.2.5 Drug Release

The IM release percentage of the PVA/SA and PVA/SA/AV unloaded and loaded hydrogels was measured after determining the encapsulation efficiency, as shown in Fig. 4.8. The IM release at two pH conditions, pH 7.4 and pH 6.4 was consistent with the swelling analysis results. At pH 7.4, the PVA/SA and PVA/SA/AV hydrogels loaded with IM exhibited a 53% and 68% release after the initial 10 mins, increasing to around 69% and 80% after 30 mins. Maximum drug release was attained after 1 hr at 78% and 81% respectively for PVA/SA and PVA/SA/AV loaded hydrogels. At pH 6.4, a higher release rate ‘burst effect’ was observed by PVA/SA/AV hydrogels. The PVA/SA and PVA/SA/AV hydrogels exhibited around 70% and 82% drug release respectively at 10 min. The release rate was further increased to 89% and 76% after 1 hr in the PVA/SA and PVA/SA/AV unloaded and loaded

hydrogel. PVA/SA/AV hydrogel achieved a maximum release rate of 94% after 24 hr. The release percentages show that adding AV in hydrogels enhances their drug release properties in a controlled pH dependant manner.

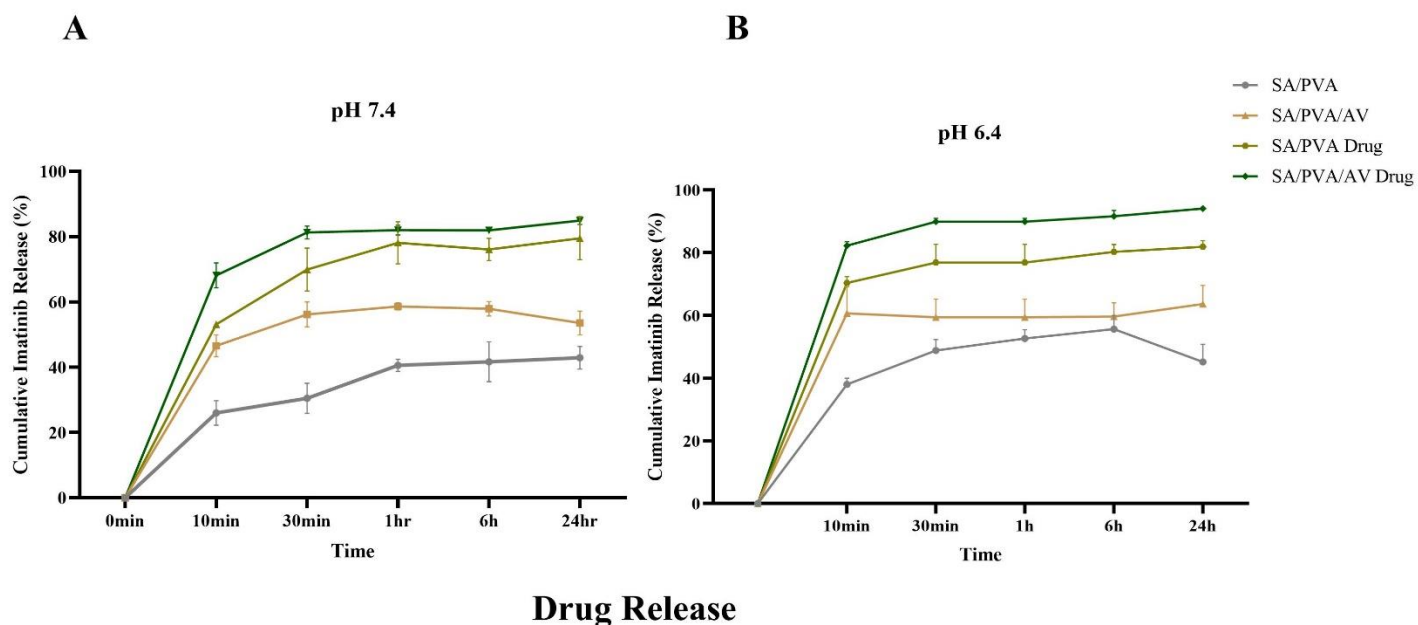


Figure 4.8 Drug Release of A) PVA/SA and PVA/SA/AV unloaded and loaded hydrogels with IM at pH 7.4, B) PVA/SA and PVA/SA/AV unloaded and loaded hydrogels with IM at pH 6.4

The standard curve was plotted at 260nm for different concentrations of IM (5 $\mu$ M, 10 $\mu$ M, 15 $\mu$ M, 20 $\mu$ M, 25 $\mu$ M, and 30 $\mu$ M). The R<sup>2</sup> value was calculated which is 0.9779. Fig 4.9.

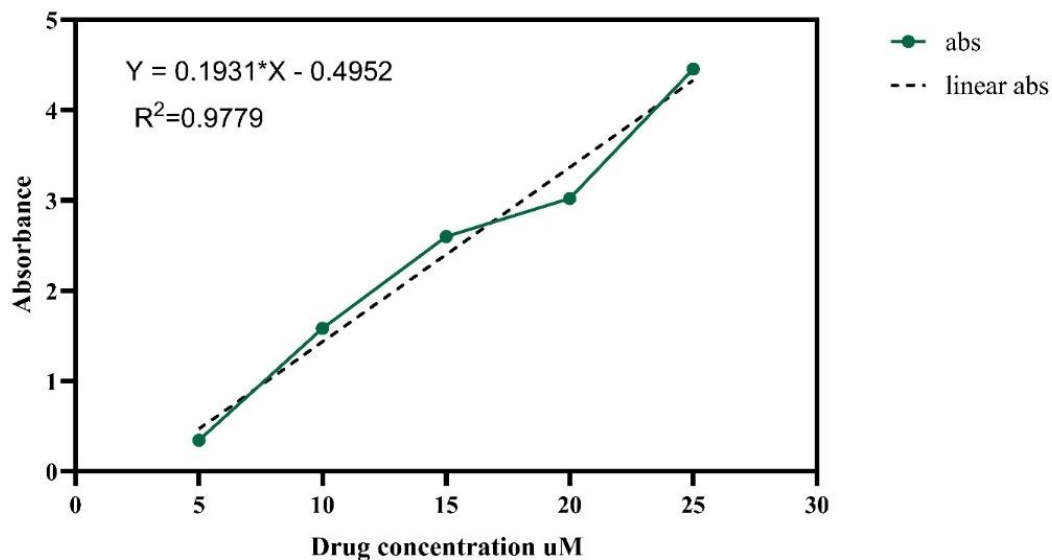
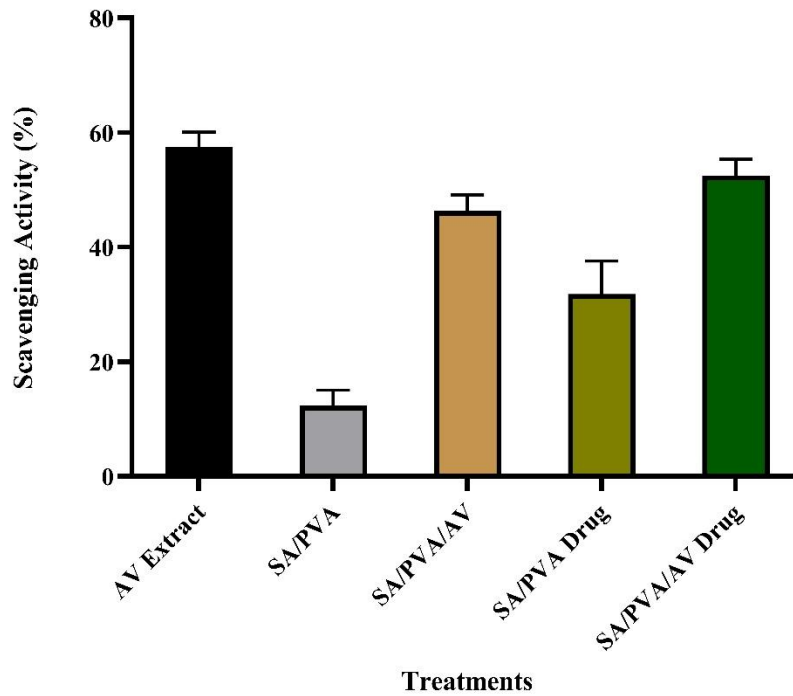


Figure 4.9 Absorbance curve and R-squared value of IM at 260nm

### 4.3 Antioxidant Analysis

The free radical scavenging activity of the PVA/SA and PVA/SA/AV hydrogels unloaded and loaded with IM were also analyzed to detect their antioxidant behavior, as shown in Fig. 4.10. The activities of the hydrogels were compared to pure AV extract as a control. 20% AV extract caused a 57% scavenging activity of the free radicals while the PVA/SA/AV hydrogel containing 20% resulted in 46% radical scavenging activity. On the other hand, the PVA/SA hydrogel loaded with IM resulted in a 32% scavenging activity. AV and IM showed a synergistic effect by increasing the antioxidant activity to 52%. The scavenging activity depends on the swelling, degradation, and release (%) of AV and IM from the hydrogel.



*Figure 4.10 Antioxidant Activity of PVA/SA and PVA/SA/AV unloaded and loaded hydrogels with IM*

#### **4.4 Biocompatibility Assay**

The biocompatibility was investigated by the hemolysis test of the PVA/SA and PVA/SA/AV hydrogels. The positive control exhibited 100% hemolysis while the negative control exhibited 0%. The PVA/SA and PVA/SA/AV hydrogels exhibited hemolysis at 3% and 2.7%, respectively, Fig. 4.11.

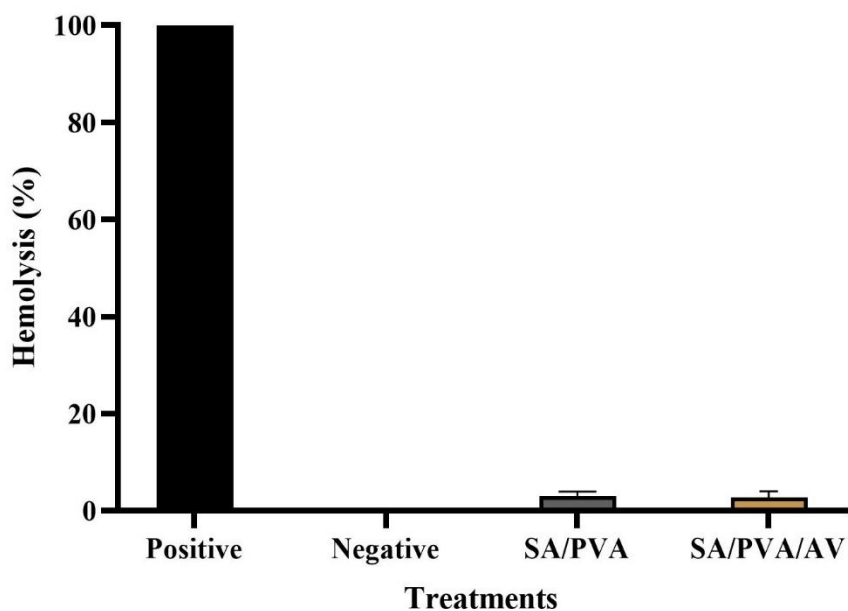


*Figure 4.11 Hemolytic Activity (%) of PVA/SA and PVA/SA/AV hydrogels*

#### **4.5 Cell Viability**

The cell proliferation and viability in cancer cells was assessed by the MTT assay, Fig 4.12. According to the analysis, IM alone resulted in 60% cell viability compared to 100% in control, which means 40% cell death was exhibited by IM. The PVA/SA/AV hydrogel exhibited almost 88% cell viability. While, the IM-loaded PVA/SA/AV hydrogel showed a significant decrease at around 40% cell viability, validating the positive outcome of incorporating IM in AV hydrogel an improved drug delivery strategy.

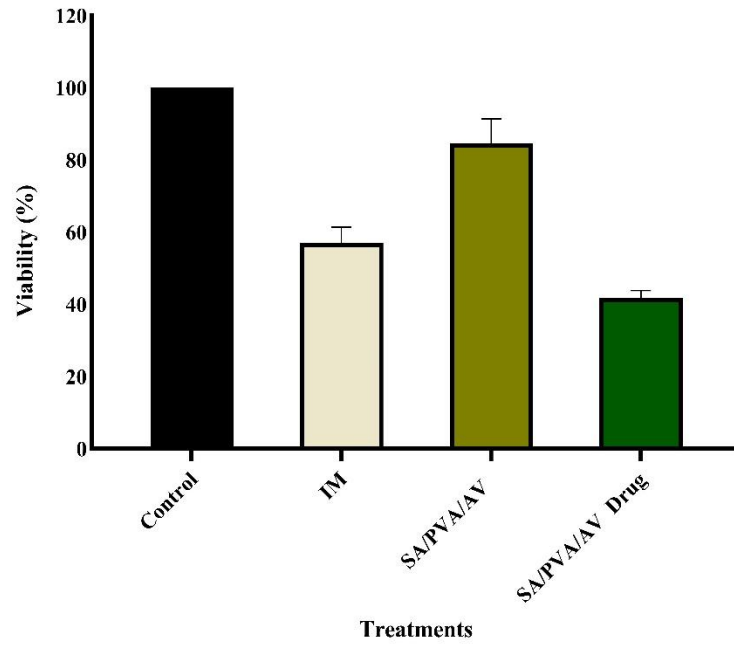


*Figure 4.12 Cell Viability PVA/SA/AV unloaded and loaded hydrogels with IM*

## CHAPTER 5: DISCUSSION

Cancer is a major health disease and the existing treatment strategies like chemotherapy and radiotherapy are limited owing to their adverse side-effects and the induction of resistance to the drugs. As a result of the limitations faced by drug DDS in cancer therapy, natural hydrogels are being explored due to their excellent physiochemical and biological features, their ability to be tuned according to the desired application, biocompatibility and biodegradability, flexibility in synthesis and drug loading and their ability to be employed in various medical applications (Jahanban-Esfahlan et al., 2020). These smart pH-based hydrogel systems have an edge over orthodox hydrogel systems and may be optimized for sustained delivery of the drugs (Zhao et al., 2022). The PVA/SA/AV hydrogels were explored for their physiochemical and biochemical properties to be employed as an efficient pH-dependent DDS in cancer.

FT-IR is performed to analyze the organic and polymeric materials for the identification of the functional and chemical groups present in the newly synthesized hydrogels. The transmittance spectrum of the PVA/SA and PVA/SA/AV hydrogels loaded and unloaded showed bands around 3000-3500  $\text{cm}^{-1}$  representing the stretching of  $-\text{OH}$  of PVA, SA, and AV whereas the intensity of the bands in AV hydrogels represents H bonding of the polysaccharides. The peak around 2930-2940  $\text{cm}^{-1}$  represents the stretching and vibrations of CH of the PVA present in the hydrogels. The  $-\text{OH}$  deformation vibrations are found between 1200-1450  $\text{cm}^{-1}$  which correspond to PVA and SA interactions with one another, leading to a more stabilized structure. The peak around 1730  $\text{cm}^{-1}$  is equivalent to the carbonyl ester peaks of AV (Bialik-Wąs, Pluta, Malina, & Majka, 2021), (Bialik-Wąs, Królicka, et al., 2021), (Bialik-Wąs, Raftopoulos, & Pielichowski, 2022), (Esposito et al., 2020). The peak at 1035  $\text{cm}^{-1}$  is equivalent to the glucan C-O and C-OH bonds of the glucans in AV and SA. The peak at 1250  $\text{cm}^{-1}$  shows the glycosidic bonds C-O-C of AV while the bands around 820  $\text{cm}^{-1}$  represent to the  $\text{CH}_2$  out of plane bending as described by (Bialik-Wąs et al., 2022). The broad peak region around 3000-3500  $\text{cm}^{-1}$  corresponds to the  $-\text{NH}$  and  $-\text{OH}$  groups of IM, whereas the C=C stretching was present around 1540  $\text{cm}^{-1}$  and C=O stretching was found around 1607  $\text{cm}^{-1}$  as confirmed by (Babu, Subha, & Rao, 2015). The characteristic intense peak at 3250  $\text{cm}^{-1}$  corresponds to the  $-\text{NH}$  stretching vibrations and C-O stretching



vibrations at  $1036\text{ cm}^{-1}$  of IM showing interaction of drug with the hydrogels (Karolewicz, Górnjak, Marciniak, & Mucha, 2019). In uncross-linked PVA, the stretching of  $\text{-OH}$  is represented at  $3253\text{ cm}^{-1}$ , while the  $\text{CH}_2$  group is represented by the vibrational bands at  $2925\text{ cm}^{-1}$ , and the  $\text{C}=\text{C}$ ,  $\text{C}-\text{C}$  stretching is prominent at  $1500\text{-}1600\text{ cm}^{-1}$  and  $837\text{ cm}^{-1}$ . The  $\text{-OH}$  hydrogen bonds contribute to the high hydrophilic properties of the PVA/AV hydrogels (Kenawy et al., 2023).

The SEM micrographs obtained presented the morphological organization of the PVA/SA/AV hydrogel and the PVA/SA/AV hydrogel loaded with IM. The ionically crosslinked PVA/SA/AV hydrogel exhibited an irregular, rough, and porous surface and cross-section with an average pore size estimated to be smaller which is similar to the literature (Bialik-Wąs et al., 2022; Kenawy et al., 2023), (Bialik-Wąs, Królicka, et al., 2021). The presence of pores is contributed by the introduction of AV in the hydrogels which increases hydrophilic ability and highly impacts swelling behavior, degradation, and drug release. In the absence of AV, dense and compact hydrogel morphology is observed, however, with the addition of 20% AV extract, the crosslinking of the hydrogels is impacted and micropores are formed (Bialik-Wąs, Pluta, Malina, & Majka, 2021). An increase in the volume of AV will decrease the crosslinking degree and increase the physiochemical properties of the hydrogels. The utilization of  $\text{CaCl}_2$  as a crosslinking agent enabled an irregular and porous structure of hydrogels. IM-functionalized galactose hydrogels exhibited smoother surfaces, compared to modified as described by (Sobierajska et al., 2023). The EDS analysis analysis confirmed the elements C, and O for PVA/SA and PVA/SA/AV hydrogels which are following the literature (Bialik-Wąs et al., 2022). The presence of Ca represents any uncrosslinked  $\text{CaCl}_2$  on the hydrogel surface. In the PVA/SA/AV hydrogel loaded with IM, the incorporation of IM was confirmed by the appearance of N in the hydrogel.

The swelling ability is largely governed by the addition of 20% AV in the hydrogels because it reduces the hydrogel crosslinking density changing its structure and morphology. As a result, the gel absorbs more water in its gel network which is consistent with our study as well (Bialik-Wąs, Pluta, Malina, & Majka, 2021). Investigation of the swelling behavior is one of the initial phases which gives us information about the release characteristics of the hydrogel. The weights of the hydrogels are obtained at different swelling conditions (pH,

temperature, salts, etc.), and the swelling ability changes with hydrogel composition and the medium, which is also consistent with our current study (Esposito et al., 2020). Another reason for the good swelling behavior of ionically cross-linked hydrogels is that SA interacts with  $\text{Ca}^{+2}$  ions to change the structure and morphology of the hydrogels which inhibits fluid absorption. Addition of 20% AV reduces the packing density of the matrix creating voids that adjust water more readily into them and also easing the release of drugs and active substances (Bialik-Wąs, Królicka, et al., 2021). The Addition of AV improves swelling behavior (Pereira, Mendes, & Bártolo, 2013). The AV hydrogels demonstrated up to 275% swelling of the hydrogel in a pH sensitive matrix with higher swelling in acidic pH and slightly lower degree of swelling in alkaline PBS, which is also analogous to our study (Bialik-Wąs et al., 2022). Additionally, the hydrogels reached maximal swelling during the early stages of the investigation, around 15-30 mins. After reaching equilibrium swelling, the hydrogel's swelling rate decreased, which could be due to the breakdown of crosslinking between SA and anions of the PBS medium, leading to the start of dissolution of the polymer and reduction in its mass (Bialik-Wąs et al., 2022). As reported by (Kenawy et al., 2023), the PVA hydrogels loaded with curcumin and gentamicin exhibited lower swelling rates while the PVA/AV hydrogels loaded with curcumin and gentamicin exhibited increased water uptake, which is also consistent with our study.

The percentage gel fraction analysis of the hydrogels influences the polymers' cross-linking behavior; the insoluble gel fraction results due to the crosslinking while the soluble fraction is due to the uncross-linked polymers, which causes weight loss (Bialik-Wąs, Pluta, Malina, Barczewski, et al., 2021). In our study, the PVA/SA unloaded and loaded hydrogels exhibited a higher gel fraction compared to the PVA/SA/AV unloaded and loaded hydrogels. The higher rate of gel fraction could be due to the formation of H bonds by PVA and its higher cross-linking capacity resulting in the stabilization of the gel, as described by (Kenawy et al., 2023). In another study by (Bialik-Wąs, Pluta, Malina, Barczewski, et al., 2021), the AV/PVA/SA hydrogels showed higher gel content compared to PVA/SA, which is in contrast to our study. This difference could be due to the utilization of ammonium persulfate as a cross-linking agent.

The degradation process of bioresorbable AV hydrogels mainly involves their disintegration into macromolecules from polymers after the breakdown of H bonds and van der Waals forces between them. The degradation is established by measuring the weight loss (%) of the hydrogels in different mediums (Bialik-Wąs, Królicka, et al., 2021). The weight loss (%) was dramatically increased upon the introduction of AV (Kenawy et al., 2023), per our study. However, the AV hydrogels developed were crosslinked in propanol which caused a 10-27% increase in degradation only, while the PVA/SA/AV hydrogels crosslinked ionically with  $\text{Ca}^{+2}$  showed a significant improvement in degradation implying the importance of crosslinking agents used in forming bioresorbable hydrogels. Additionally, stronger degradation (%) at the higher pH results from the ionization of the carboxylate groups in SA which loosens up the crosslinking, facilitating swelling and consequently speeding up the progression of degradation (Bialik-Wąs, Pluta, Malina, & Majka, 2021).

The drug entrapment efficiency of IM in poly(lactic) acid (PLA) microspheres was investigated to be at 64.24% while the collagen coated microspheres were found to be 59.42% in a study which is similar to the entrapment efficiency obtained by IM in our study (Babu et al., 2015). In one study, the loading of AV in niosomes was found to be 42% (Dadashzadeh et al., 2020). The loading of the drug in nanoparticles was found to be 43.3% (Bhullar, Goyal, & Gupta, 2022). The drug release profile of the PVA/SA and PVA/SA/AV unloaded and loaded with IM hydrogels was also investigated. A ‘burst effect’ release of IM was observed in loaded PVA/SA and PVA/SA/AV hydrogels in pH 6.4, which is consistent with another study where maximum AV was released within 120min and the highest concentration release was achieved within 24h (Bialik-Wąs, Królicka, et al., 2021). As mentioned above, the physical crosslinking of the hydrogels enables rapid swelling and release of the drug into the PBS solution, from the matrix. The pulsative or burst release can also be associated with matrix changes (Bialik-Wąs, Królicka, et al., 2021). In a similar study, a sustained and controlled release of IM was achieved from nanoparticles at lower pH which resulted in a faster release than neutral pH conditions which could be due to the faster degradation of the nanoparticles at lower pH (Bhullar et al., 2022). This reduces the chance of adverse side effects after drug delivery. IM was also observed to be released 100% from the IM-functionalized galactose hydrogels within 1h, as described by (Sobierajska et al., 2023). Additionally, gentamicin was also observed to be released from PVA/AV hydrogel

membranes rapidly around 40% to 90% within the first 15min of the analysis. It was suggested that the burst release was associated with the drug being loaded near the surface of the membrane. Increasing the concentration of AV increased the release profile due to the development of a spongy porous matrix. A high concentration of AV facilitates the loading of the drug. As a result, a controlled release is established due to the high swellability of the hydrogel which is also seen in our study (Kenawy et al., 2023).

The DPPH helped analyze the ROS scavenging activity of AV and IM in combination. The ROS levels increase in cancerous cells due to the antioxidant activity which can cause toxicity in the system. The PVA/SA/AV hydrogels exhibited a synergistic effect with IM, increasing the antioxidant activity. The scavenging activity of IM is previously reported to be 83.3%, while under the influence of glucose, it is found to be 70%, with a 13% decrease (Sabina & Ameta, 2023). In a similar study, the incorporation of quercetin in PVA/SA hydrogels reduced the antioxidant activity (Esposito et al., 2020), which can also justify the activity of PVA/SA/AV hydrogel loaded with IM at 56%. The cross-linking percentage, swelling, release, and incubation period all affect the scavenging activity (%).

The hydrogels are tested for their biocompatibility through the hemolytic assay, as the interaction of the hydrogel might cause hemoglobin leakage due to a compromise in the membrane integrity of the RBCs (Bhoopathy et al., 2024). The PVA/SA and PVA/SA/AV hydrogels, both showed hemolytic percentage less than 5% verifying the non-hemolytic and good biocompatible nature of the hydrogels as shown by (Kenawy et al., 2023).

The cell viability analysis of the unloaded and IM loaded PVA/SA/AV hydrogels was investigated through the MTT assay. The increase in cell viability in PVA/SA/AV unloaded hydrogels is due to the proliferative and biocompatible nature of AV, as suggested by (Dadashzadeh et al., 2020). In one reported study, the addition of AV did not affect the cytotoxicity of chitosan-based hydrogels, according to the ISO standards which state that a compound is deemed cytotoxic if the cell viability is less than 70% after 24h of treatment (Kudłacik-Kramarczyk et al., 2021). This is also true for our study as the viability was found to be greater than 80%. However, our study suggested that in combination with IM, the AV

hydrogels caused a synergistic effect reducing the cell viability to 40% which was nearly 56% with IM alone.

## **CHAPTER 6: CONCLUSION AND FUTURE PROSPECTS**

The drug delivery systems have seen a surge in their investigations for their potential in anti-cancer treatment strategies. A considerable drug delivery system can avoid the toxication of healthy cells, elimination of drugs from the body, and undesirable circulation in the blood. They can act as reservoirs for controlled and sustained encapsulation and release of the drug from the hydrogel system. In our current study, we were able to achieve considerable encapsulation of the anticancer drug into the AV hydrogel system with structural stability, followed by pH-controlled release and promising results in the anticancer activity; decreased drug resistance, and increased cytotoxicity. In the future, hydrogel based DDS can be used in the development of systems for cancer therapy, immunotherapy, gene therapy, etc. The release kinetics can be more precisely controlled in-vitro for further testing in-vivo leading to clinical trials. Additionally, there exist some drawbacks which act as a limitation in clinical trials. These limitations like size, charge, long-acting drug incorporation, scaling up, reproducibility, etc. are to be addressed by the development of pre-clinical models before jumping toward clinical trials.

## REFERENCES

- Abbas, G., Shah, S., Hanif, M., Asghar, A., Shafique, M., & Ashraf, K. J. B. C. (2020). Cancer prevalence, incidence and mortality rates in Pakistan in 2018. *Bull Cancer*, *107*(4), 517-518.
- Afshar, M., Dini, G., Vaezifar, S., Mehdikhani, M., Movahedi, B. J. J. o. D. D. S., & Technology. (2020). Preparation and characterization of sodium alginate/polyvinyl alcohol hydrogel containing drug-loaded chitosan nanoparticles as a drug delivery system. *Journal of Drug Delivery* *56*, 101530.
- Ahmed, E. M. J. J. o. a. r. (2015). Hydrogel: Preparation, characterization, and applications: A review. *Journal of Advanced Research*, *6*(2), 105-121.
- Ali, A., Manzoor, M. F., Ahmad, N., Aadil, R. M., Qin, H., Siddique, R., . . . Khalid, W. J. F. i. n. (2022). The burden of cancer, government strategic policies, and challenges in Pakistan: A comprehensive review. *Frontiers in nutrition*, *9*, 940514.
- Ashouri, F., Beyranvand, F., Beigi Boroujeni, N., Tavafi, M., Sheikhan, A., Varzi, A. M., . . . research, t. (2019). Macrophage polarization in wound healing: role of aloe vera/chitosan nanohydrogel. *Drug delivery and translational research*, *9*, 1027-1042.
- Babu, C., Subha, M., & Rao, K. C. J. I. J. D. D. (2015). Controlled delivery of imatinib mesylate from collagen coated poly (lactic acid) microspheres: in vitro release studies. *International Journal of Drug Delivery*, *6*, 373-379.
- Balaji, A., Vellayappan, M. V., John, A. A., Subramanian, A. P., Jaganathan, S. K., SelvaKumar, M., . . . Yusof, M. J. R. a. (2015). Biomaterials based nano-applications of Aloe vera and its perspective: a review. *RSC advances*, *5*(105), 86199-86213.
- Bhoopathy, J., Vedakumari Sathyaraj, W., Yesudhasan, B. V., Rajendran, S., Dharmalingam, S., Seetharaman, J., . . . Anandasadagopan, S. K. (2024). Haemostatic potency of sodium alginate/aloe vera/sericin composite scaffolds – preparation, characterisation, and evaluation. *Artificial Cells, Nanomedicine, and Biotechnology*, *52*(1), 35-45. doi:10.1080/21691401.2023.2293784
- Bhullar, S., Goyal, N., & Gupta, S. (2022). In-vitro pH-responsive release of imatinib from iron-supplement coated anatase TiO(2) nanoparticles. *Sci Rep*, *12*(1), 4600. doi:10.1038/s41598-022-08090-7
- Bialik-Wąs, K., Królicka, E., & Malina, D. J. M. (2021). Impact of the type of crosslinking agents on the properties of modified sodium alginate/poly (vinyl alcohol) hydrogels. *Molecules*, *26*(8), 2381.
- Bialik-Wąs, K., Pielichowski, K. J. I. J. o. P. M., & Biomaterials, P. (2018). Bio-hybrid acrylic hydrogels containing metronidazole-loaded poly (acrylic acid-co-methyl

methacrylate) nanoparticles and Aloe vera as natural healing agent. *International Journal of Polymeric Materials and Polymeric Biomaterials*.

- Bialik-Wąs, K., Pluta, K., Malina, D., Barczewski, M., Malarz, K., Mrozek-Wilczkiewicz, A. J. M. S., & C, E. (2021). Advanced SA/PVA-based hydrogel matrices with prolonged release of Aloe vera as promising wound dressings. *Materials Science and Engineering*, 120, 111667.
- Bialik-Wąs, K., Pluta, K., Malina, D., & Majka, T. M. (2021). Alginate/PVA-based hydrogel matrices with Echinacea purpurea extract as a new approach to dermal wound healing. *International Journal of Polymeric Materials and Polymeric Biomaterials*, 70(3), 195-206. doi:10.1080/00914037.2019.1706510
- Bialik-Wąs, K., Raftopoulos, K. N., & Pieliowski, K. J. M. (2022). Alginate hydrogels with aloe vera: the effects of reaction temperature on morphology and thermal properties. *Materials*, 15(3), 748.
- Birgisson, H., Páhlman, L., Gunnarsson, U., & Glimelius, B. J. A. o. (2007). Late adverse effects of radiation therapy for rectal cancer—a systematic overview. *Acta oncologica*, 46(4), 504-516.
- Bordbar-Khiabani, A., & Gasik, M. J. I. J. o. M. S. (2022). Smart hydrogels for advanced drug delivery systems. *International Journal of Molecular Sciences*, 23(7), 3665.
- Burgess, M. R., & Sawyers, C. L. J. T. S. W. J. (2006). Treating Imatinib-Resistant Leukemia: The Next Generation Targeted Therapies. *The Scientific World Journal*, 6(1), 918-930.
- Cairns, J. J. S. A. (1975). The cancer problem. *Scientific American*, 233(5), 64-79.
- Capes-Davis, A., Theodosopoulos, G., Atkin, I., Drexler, H. G., Kohara, A., MacLeod, R. A., . . . Reddel, R. R. J. I. j. o. c. (2010). Check your cultures! A list of cross-contaminated or misidentified cell lines. *International journal of cancer*, 127(1), 1-8.
- Chang, X., Zhao, J., Tian, F., Jiang, Y., Lu, J., Ma, J., . . . Dong, Z. J. O. I. (2016). Aloe-emodin suppresses esophageal cancer cell TE1 proliferation by inhibiting AKT and ERK phosphorylation. *Oncology letters*, 12(3), 2232-2238.
- Chelu, M., Musuc, A. M., Popa, M., & Calderon Moreno, J. J. G. (2023). Aloe vera-based hydrogels for wound healing: Properties and therapeutic effects. *Gels*, 9(7), 539.
- Chen, Q., Li, K.-T., Tian, S., Yu, T.-H., Yu, L.-H., Lin, H.-D., . . . treatment. (2018). Photodynamic therapy mediated by aloe-emodin inhibited angiogenesis and cell metastasis through activating MAPK signaling pathway on HUVECs. *Technology in cancer research & treatment*, 17, 1533033818785512.
- Dadashzadeh, A., Imani, R., Moghassemi, S., Omidfar, K., & Abolfathi, N. (2020). Study of hybrid alginate/gelatin hydrogel-incorporated niosomal Aloe vera capable of sustained



release of Aloe vera as potential skin wound dressing. *Polymer Bulletin*, 77(1), 387-403. doi:10.1007/s00289-019-02753-8

- Dannert, C., Stokke, B. T., & Dias, R. S. J. P. (2019). Nanoparticle-hydrogel composites: from molecular interactions to macroscopic behavior. *Polymers*, 11(2), 275.
- Dattilo, M., Patitucci, F., Prete, S., Parisi, O. I., & Puoci, F. J. J. o. F. B. (2023). Polysaccharide-based hydrogels and their application as drug delivery systems in cancer treatment: a review. *Journal of functional biomaterials*, 14(2), 55.
- Deen, G. R., & Loh, X. J. J. G. (2018). Stimuli-responsive cationic hydrogels in drug delivery applications. *Gels*, 4(1), 13.
- Esposito, L., Barbosa, A. I., Moniz, T., Costa Lima, S., Costa, P., Celia, C., & Reis, S. (2020). Design and Characterization of Sodium Alginate and Poly(vinyl) Alcohol Hydrogels for Enhanced Skin Delivery of Quercetin. *Pharmaceutics*, 12(12), 1149.
- Ghasemiyeh, P., & Mohammadi-Samani, S. J. T. i. p. s. (2019). Hydrogels as drug delivery systems; pros and cons. *Trends in pharmaceutical sciences*, 5(1), 7-24.
- Gonçalves, C., Pereira, P., & Gama, M. J. M. (2010). Self-assembled hydrogel nanoparticles for drug delivery applications. *Materials*, 3(2), 1420-1460.
- Holliday, D. L., & Speirs, V. J. B. c. r. (2011). Choosing the right cell line for breast cancer research. *Breast cancer research*, 13, 1-7.
- Hussain, A., Sharma, C., Khan, S., Shah, K., & Haque, S. J. A. P. J. o. C. P. (2015). Aloe vera inhibits proliferation of human breast and cervical cancer cells and acts synergistically with cisplatin. *Asian Pacific Journal of Cancer Prevention*, 16(7), 2939-2946.
- Ishfaq, B., Khan, I. U., Khalid, S. H., & Asghar, S. (2023). Design and evaluation of sodium alginate-based hydrogel dressings containing *Betula utilis* extract for cutaneous wound healing. *Front Bioeng Biotechnol*, 11, 1042077. doi:10.3389/fbioe.2023.1042077
- Jacob, S., Nair, A. B., Shah, J., Sreeharsha, N., Gupta, S., & Shinu, P. J. P. (2021). Emerging role of hydrogels in drug delivery systems, tissue engineering and wound management. *Pharmaceutics*, 13(3), 357.
- Jahanban-Esfahlan, R., Derakhshankhah, H., Haghshenas, B., Massoumi, B., Abbasian, M., & Jaymand, M. J. I. j. o. b. m. (2020). A bio-inspired magnetic natural hydrogel containing gelatin and alginate as a drug delivery system for cancer chemotherapy. *International journal of biological macromolecules*, 156, 438-445.
- Jain, K. K. (2020). Role of Nanobiotechnology in Drug Delivery. In K. K. Jain (Ed.), *Drug Delivery Systems* (pp. 55-73). New York, NY: Springer New York.

- Jiang, Y., Krishnan, N., Heo, J., Fang, R. H., & Zhang, L. J. J. o. C. R. (2020). Nanoparticle–hydrogel superstructures for biomedical applications. *Journal of Controlled Release*, 324, 505-521.
- Karolewicz, B., Górniak, A., Marciniak, D. M., & Mucha, I. J. P. (2019). Molecular mobility and stability studies of amorphous imatinib mesylate. *Pharmaceutics*, 11(7), 304.
- Kenawy, E.-R. S., Kamoun, E. A., Ghaly, Z. S., Shokr, A.-b. M., El-Meligy, M. A., Mahmoud, Y. A.-G. J. A. J. f. S., & Engineering. (2023). Novel physically cross-linked curcumin-loaded PVA/aloe vera hydrogel membranes for acceleration of topical wound healing: In vitro and in vivo experiments. *Arabian Journal for Science and Engineering*, 48(1), 497-514.
- Ketabat, F., Pundir, M., Mohabatpour, F., Lobanova, L., Koutsopoulos, S., Hadjiiski, L., . . . Papagerakis, S. J. P. (2019). Controlled drug delivery systems for oral cancer treatment—current status and future perspectives. *Pharmaceutics*, 11(7), 302.
- Khani, A., Eskandani, M., Derakhshankhah, H., Soleimani, K., Nakhjavani, S. A., Massoumi, B., . . . Jaymand, M. J. J. o. P. R. (2022). A novel stimuli-responsive magnetic hydrogel based on nature-inspired tragacanth gum for chemo/hyperthermia treatment of cancerous cells. *Journal of Polymer Research*, 29(4), 149.
- Khursheed, R., Dua, K., Vishwas, S., Gulati, M., Jha, N. K., Aldhafeeri, G. M., . . . pharmacotherapy. (2022). Biomedical applications of metallic nanoparticles in cancer: Current status and future perspectives. *Biomedicine & pharmacotherapy*, 150, 112951.
- Kim, J. I., Kim, B., Chun, C., Lee, S. H., & Song, S.-C. J. B. (2012). MRI-monitored long-term therapeutic hydrogel system for brain tumors without surgical resection. *Biomaterials*, 33(19), 4836-4842.
- Klein, A. D., & Penneys, N. S. J. J. o. t. A. A. o. D. (1988). Aloe vera. *Journal of the American Academy of Dermatology*, 18(4), 714-720.
- Kudłacik-Kramarczyk, S., Drabczyk, A., Głab, M., Alves-Lima, D., Lin, H., Douglas, T., . . . C, E. (2021). Investigations on the impact of the introduction of the Aloe vera into the hydrogel matrix on cytotoxic and hydrophilic properties of these systems considered as potential wound dressings. *Materials Science and Engineering*, 123, 111977.
- Liu, Y.-q., Meng, P.-s., Zhang, H.-c., Liu, X., Wang, M.-x., Cao, W.-w., . . . Pharmacotherapy. (2018). Inhibitory effect of aloe emodin mediated photodynamic therapy on human oral mucosa carcinoma in vitro and in vivo. *Biomedicine*, 97, 697-707.
- Ma, W., Chen, Q., Xu, W., Yu, M., Yang, Y., Zou, B., . . . Yu, Z. J. N. R. (2021). Self-targeting visualizable hyaluronate nanogel for synchronized intracellular release of doxorubicin and cisplatin in combating multidrug-resistant breast cancer. *Nano Research*, 14, 846-857.

- Martinez-Garcia, F. D., Fischer, T., Hayn, A., Mierke, C. T., Burgess, J. K., & Harmsen, M. C. J. G. (2022). A beginner's guide to the characterization of hydrogel microarchitecture for cellular applications. *Gels*, 8(9), 535.
- Mattiuzzi, C., Lippi, G. J. J. o. e., & health, g. (2019). Current cancer epidemiology. 9(4), 217-222.
- Mehlen, P., & Puisieux, A. J. N. r. c. (2006). Metastasis: a question of life or death. *Nature Reviews Cancer*, 6(6), 449-458.
- Mohan, G., TP, A. H., AJ, J., KM, S. D., Narayanasamy, A., Vellingiri, B. J. T. J. o. B., & Zoology, A. (2019). Recent advances in radiotherapy and its associated side effects in cancer—a review. *The Journal of Basic and Applied Zoology*, 80(1), 1-10.
- Moschovi, M., & Kelaidi, C. J. I. J. o. M. S. (2021). Chronic Myeloid Leukemia in Children and Adolescents: The Achilles Heel of Oncogenesis and Tyrosine Kinase Inhibitors. *International Journal of Molecular Sciences*, 22(15), 7806.
- Nasef, S. M., Khozemy, E. E., & Mahmoud, G. A. J. S. R. (2023). pH-responsive chitosan/acrylamide/gold/nanocomposite supported with silver nanoparticles for controlled release of anticancer drug. *Scientific Reports*, 13(1), 7818.
- Nazir, S., Khan, M. U. A., Al-Arjan, W. S., Abd Razak, S. I., Javed, A., & Kadir, M. R. A. J. A. J. o. C. (2021). Nanocomposite hydrogels for melanoma skin cancer care and treatment: In-vitro drug delivery, drug release kinetics and anti-cancer activities. *Arabian Journal of Chemistry*, 14(5), 103120.
- O'Dwyer, M. J. T. O. (2002). Multifaceted approach to the treatment of bcr-abl-positive leukemias. *The Oncologist*, 7(S1), 30-38.
- Pacheco, C., Baiao, A., Ding, T., Cui, W., & Sarmiento, B. J. A. D. D. R. (2023). Recent advances in long-acting drug delivery systems for anticancer drug. *Advanced Drug Delivery Reviews*, 194, 114724.
- Park, K. M., Lewis, D., & Gerecht, S. J. A. r. o. b. e. (2017). Bioinspired hydrogels to engineer cancer microenvironments. *ANNUAL REVIEW OF BIOMEDICAL ENGINEERING*, 19, 109-133.
- Pereira, R., Mendes, A., & Bártolo, P. (2013). Alginate/Aloe Vera Hydrogel Films for Biomedical Applications. *Procedia CIRP*, 5, 210-215. doi:<https://doi.org/10.1016/j.procir.2013.01.042>
- Puranik, A. S., Pao, L. P., White, V. M., Peppas, N. A. J. E. J. o. P., & Biopharmaceutics. (2016). Synthesis and characterization of pH-responsive nanoscale hydrogels for oral delivery of hydrophobic therapeutics. *European Journal of Pharmaceutics and Biopharmaceutics*, 108, 196-213.

- Rahman, S., Carter, P., & Bhattarai, N. J. J. o. f. b. (2017). Aloe vera for tissue engineering applications. *Journal of functional biomaterials*, 8(1), 6.
- Rivera-Hernández, G., Antunes-Ricardo, M., Martínez-Morales, P., & Sanchez, M. L. J. I. J. o. P. (2021). Polyvinyl alcohol based-drug delivery systems for cancer treatment. *International Journal of Pharmaceutics*, 600, 120478.
- Sabina, & Ameta, R. K. (2023). Effect of glucose on anti-oxidant activity of Morin and Imatinib mesylate estimated through spectrophotometric and physicochemical analysis. *Journal of Molecular Liquids*, 387, 122714. doi:<https://doi.org/10.1016/j.molliq.2023.122714>
- Sadgrove, N. J., & Simmonds, M. S. J. P. R. (2021). Pharmacodynamics of Aloe vera and acemannan in therapeutic applications for skin, digestion, and immunomodulation. *Phytotherapy Research*, 35(12), 6572-6584.
- Sánchez-Machado, D. I., López-Cervantes, J., Sendón, R., Sanches-Silva, A. J. T. i. F. S., & Technology. (2017). Aloe vera: Ancient knowledge with new frontiers. *Trends in Food Science & Technology*, 61, 94-102.
- Sánchez, M., González-Burgos, E., Iglesias, I., & Gómez-Serranillos, M. P. J. M. (2020). Pharmacological update properties of Aloe vera and its major active constituents. *Molecules*, 25(6), 1324.
- Sepantafar, M., Maheronnaghsh, R., Mohammadi, H., Radmanesh, F., Hasani-Sadrabadi, M. M., Ebrahimi, M., & Baharvand, H. J. T. i. b. (2017). Engineered hydrogels in cancer therapy and diagnosis. *Trends in Biotechnology*, 35(11), 1074-1087.
- Siegel, R. L., Miller, K. D., Wagle, N. S., & Jemal, A. J. C. C. J. C. (2023). Cancer statistics, 2023. *A Cancer Journal for Clinicians*, 73(1), 17-48.
- Sobierajska, P., Wiatrak, B., Jawien, P., Janeczek, M., Wiglusz, K., Szelağ, A., & Wiglusz, R. J. J. A. o. (2023). Imatinib-Functionalized Galactose Hydrogels Loaded with Nanohydroxyapatite as a Drug Delivery System for Osteosarcoma: In Vitro Studies. *ACS omega*, 8(20), 17891-17900.
- Sogawa, C., Eguchi, T., Namba, Y., Okusha, Y., Aoyama, E., Ohyama, K., & Okamoto, K. J. C. (2021). Gel-free 3D tumoroids with stem cell properties modeling drug resistance to cisplatin and imatinib in metastatic colorectal cancer. *Cells*, 10(2), 344.
- Sullad, A. G., Manjeshwar, L. S., Aminabhavi, T. M. J. I., & Research, E. C. (2010). Novel pH-sensitive hydrogels prepared from the blends of poly (vinyl alcohol) with acrylic acid-graft-guar gum matrixes for isoniazid delivery. *Industrial & Engineering Chemistry Research* 49(16), 7323-7329.

- Sun, Z., Song, C., Wang, C., Hu, Y., & Wu, J. J. M. p. (2019). Hydrogel-based controlled drug delivery for cancer treatment: a review. *Molecular pharmaceuticals*, 17(2), 373-391.
- Ta, H. T., Dass, C. R., & Dunstan, D. E. J. J. o. C. R. (2008). Injectable chitosan hydrogels for localised cancer therapy. *Journal of Controlled Release*, 126(3), 205-216.
- Tian, R., Chen, J., & Niu, R. J. N. (2014). The development of low-molecular weight hydrogels for applications in cancer therapy. *Nanoscale*, 6(7), 3474-3482.
- Wang, Y., Zhang, Y., Lin, Z., Huang, T., Li, W., Gong, W., . . . Tu, Q. J. C. P. B. E. (2021). A green method of preparing a natural and degradable wound dressing containing aloe vera as an active ingredient. *Composites Part B: Engineering*, 222, 109047.
- Yang, K., Han, Q., Chen, B., Zheng, Y., Zhang, K., Li, Q., & Wang, J. J. I. J. o. N. (2018). Antimicrobial hydrogels: promising materials for medical application. *International Journal of Nanomedicine*, 2217-2263.
- Zhao, Y., Ran, B., Xie, X., Gu, W., Ye, X., & Liao, J. J. G. (2022). Developments on the Smart Hydrogel-Based Drug Delivery System for Oral Tumor Therapy. *Gels*, 8(11), 741.
- Zhu, J., & Marchant, R. E. J. E. r. o. m. d. (2011). Design properties of hydrogel tissue-engineering scaffolds. *Expert review of medical devices*, 8(5), 607-626.